Extraction, purification, and clumped isotope analysis of methane ($\Delta^{13}CDH_3$ and $\Delta^{12}CD_2H_2$) from sources and the atmosphere

Malavika Sivan, Thomas Röckmann, Carina van der Veen, Maria Elena Popa

Institute for Marine and Atmospheric Research Utrecht (IMAU), Utrecht University, the Netherlands

Correspondence to: Malavika Sivan (m.sivan@uu.nl)

Abstract

Measurements of the clumped isotope anomalies ($\Delta^{13}CDH_3$ and $\Delta^{12}CD_2H_2$) of methane have shown potential for constraining methane sources and sinks. At Utrecht University, we use the Thermo Ultra high-resolution isotope ratio mass spectrometer to measure the clumped isotopic composition of methane emitted from various sources and directly from the atmosphere.

We have developed an extraction system with three sections for extracting and purifying methane from high (>1 %), medium (0.1-1 %), and low-concentration (< 1 %) samples, including atmospheric air (~2 ppm = 0.0002 %). Depending on the methane concentration, a quantity of sample gas is processed that delivers 3 ± 1 mL of pure methane, which is the quantity typically needed for one clumped isotope measurement. For atmospheric air with a methane mole fraction of 2 ppm, we currently process up to 1100 L of air.

The analysis is performed on pure methane, using a dual inlet setup. The complete measurement time for all isotope signatures is about 20 hours for one sample. The mean internal precision of sample measurements is 0.3 ± 0.1 ‰ for $\Delta^{13}CDH_3$ and 2.4 ± 0.8 ‰ for $\Delta^{12}CD_2H_2$. The long-term reproducibility, obtained from repeated measurements of a constant target gas, over almost 3 years, is around 0.15 ‰ for $\Delta^{13}CDH_3$ and 1.2 ‰ for $\Delta^{12}CD_2H_2$. The measured clumping anomalies are calibrated via the $\Delta^{13}CDH_3$ and $\Delta^{12}CD_2H_2$ values of the reference CH_4 used for the dual inlet measurements. These were determined through isotope equilibration experiments at temperatures between 50 and 450 °C.

We describe in detail the optimized sampling, extraction, purification, and measurement technique followed in our laboratory to measure the clumping anomalies of methane precisely and accurately. This paper highlights the extraction and one of the first global measurements of the clumping anomalies of atmospheric methane.

1. Introduction

Atmospheric methane, CH_4, is the second most important anthropogenic greenhouse gas after CO_2. The global warming potential of CH_4 is 28 times greater than that of CO_2 over a 100-

year period. Having a shorter lifetime of ~11 years (Li et al., 2022) compared to CO_2 (Archer et al., 2009), CH_4 responds faster to changes in its source and sink fluxes than CO_2. This also means that CH_4 emission reduction measures can have a relatively faster effect on atmospheric composition, reducing global warming. Global scale measurements of CH_4 mole fractions show an increasing trend since pre-industrial times. The current global mean atmospheric CH_4 mole fraction as of January 2023 is 1972 ppb while the estimated pre-industrial values were 700-800 ppb (NOAA 2023). This long-term increase is mostly attributed to anthropogenic emissions (IPCC 2022). Precise direct atmospheric measurements have revealed significant shorter-term variations in the growth rate of atmospheric CH_4, including stable levels in the early 2000s followed by an accelerating increase since 2007. Various studies have attempted to attribute this temporal change to variations in the balance between different CH_4 sources and atmospheric sinks. However, these existing studies do not converge on the same conclusion. This shows we don't fully understand the CH_4 cycle yet, which means that we cannot predict its future behaviour confidently.

Major CH_4 sources are often separated into these categories according to the production mechanism: biogenic (wetlands, cattle, lakes, landfills), thermogenic (natural gas, coalbed CH_4, shale gas, etc), pyrogenic (biomass burning, combustion of fossil fuels, etc.) and abiotic (volcanic and geothermal areas, gas-water-rock interactions etc) sources. The main CH_4 sink in the troposphere is photochemical oxidation by OH and Cl radicals (Khalil et al., 1993). Part of the CH_4 that reaches the stratosphere is removed by Cl and $O(^1D)$. About 10 % of the atmospheric CH_4 is taken up by surface sinks (Topp and Pattey, 1997).

A method commonly used to identify different sources and sinks of CH_4 is based on measurements of its bulk isotopic composition, denoted as $\delta^{13}C$ and δD. Each source has a characteristic isotopic composition range as shown in Fig 1a, as a result of the isotopic composition of the various substrates and the process-dependent isotopic fractionation during CH_4 formation (Whiticar et al., 1986; Whiticar, 1999; Sherwood Lollar et al., 2006; Etiope and Sherwood Lollar, 2013; Conrad, 2002; Kelly et al., 2022; Menoud et al., 2020). CH_4 from all these sources contribute to atmospheric CH_4 with an expected isotopic composition of the source mixture around -54 ‰ for $\delta^{13}C$ and -290 ‰ for δD (Whiticar and Schaefer, 2007) (as shown in Fig 1a). The sink reactions preferentially remove the lighter isotopologues of CH_4 from the atmosphere (Saueressig et al., 2001; Cantrell et al., 1990; Whitehill et al., 2017) resulting in an enrichment of the heavier isotopes in the residual CH_4. The combined effect of emissions from the various sources and removal by the different sinks lead to an overall atmospheric CH_4 bulk isotopic composition of around -48 ‰ for $\delta^{13}C$ and -90 ‰ for δD. Many measurements have been performed to date, using analysis in the laboratory on collected samples, and field-deployable instruments at various sites to study the variations in atmospheric CH_4 (Menoud et al., 2020; Menoud et al., 2021; Menoud et al., 2022; Lu et al., 2021; Beck et al., 2012; Fernandez et al., 2022; Röckmann et al., 2016b; Sherwood et al., 2017). However, due to the overlap of some of the source signatures, it is not always possible to distinguish different sources of CH_4 using the bulk isotopes (Fig 1a).

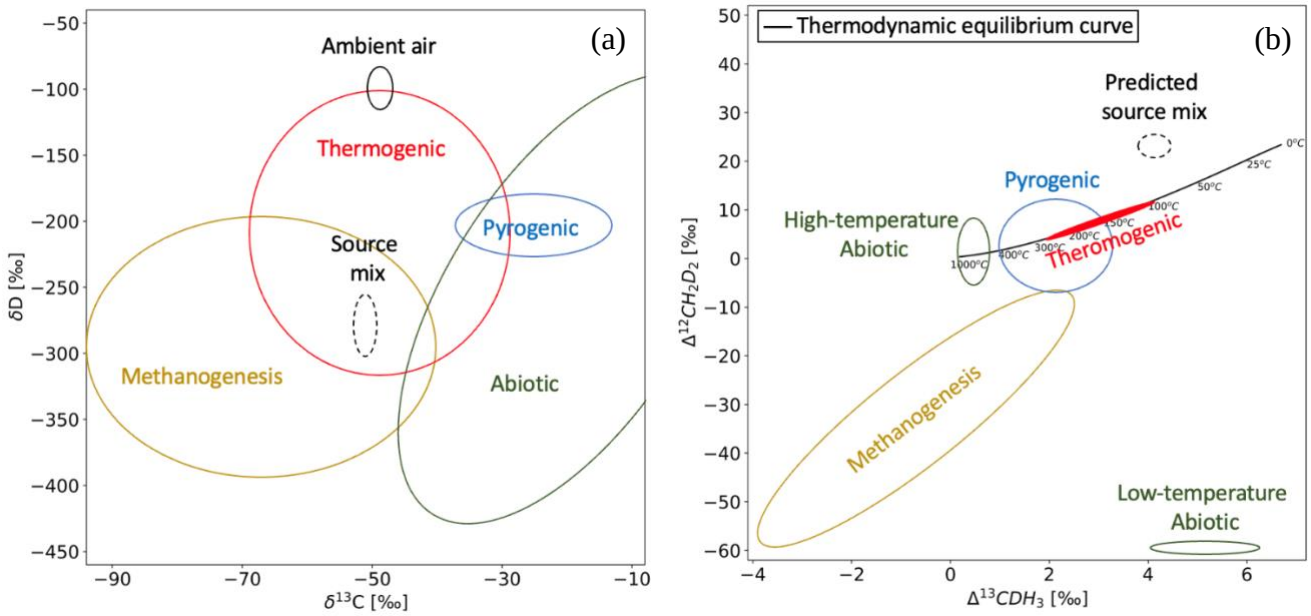

Fig 1: An illustration of bulk (a) and clumped (b) isotopic composition of major CH_4 sources as reported so far.

The measurement of the two most abundant clumped isotopologues ($^{13}CDH_3$ and $^{12}CD_2H_2$) of CH_4 can be used as an additional tool to constrain CH_4 sources (Douglas et al., 2017; Eiler, 2007; Young et al., 2017; Stolper et al., 2014). The clumping anomalies, denoted as $\Delta^{13}CDH_3$ and $\Delta^{12}CD_2H_2$, are a measure of the deviation of the number of clumped molecules present relative to that expected from the random distribution of the light and heavy isotopes over all isotopologues of CH_4. At thermodynamic equilibrium, these anomalies are temperature-dependent and can thus be used to calculate the CH_4 formation or equilibration temperature. In the case of thermodynamic disequilibrium, the clumped signatures can be exploited to identify various kinetic gas formation and fractionation (mixing, diffusion, etc.) processes. The clumped isotope signatures are specific to different sources and processes, independent of the bulk signatures, and thus can deliver additional information on sources and cycling of CH_4 in the environment.

Measuring the clumped isotopic composition of CH_4, however, poses several technical challenges. The $^{13}CDH_3$ and CD_2H_2 molecules and H_2O (which is always present in a mass spectrometer at much higher concentrations than the CH_4 clumped isotopologues) have very slightly different masses, approximately 18.0409, 18.0439 and 18.0153 atomic mass units, respectively. This difference cannot be distinguished using a conventional mass spectrometer. Also, the $^{13}CH_4$ and CDH_3 have the same nominal mass (m/z 17), but these interferences can be circumvented by separating the C and H atoms, i.e., by converting the CH_4 to CO_2 for the $\delta^{13}C$ measurements, and to H_2 for δD. For clumped isotope measurements such an approach would eliminate the signal we are looking for, thus the measurements need to be performed on intact CH_4 molecules. In recent years, high-resolution isotope ratio mass spectrometers have become available that can resolve these small mass differences (Eiler et al., 2013; Young et al., 2017). These new instruments can separate the ion beams around mass 18

corresponding to CH_3D^+, $^{12}CH_2D_2^+$ and $H_2{}^{16}O^+$ facilitating the CH_4 clumped isotope measurements.

Another challenge includes the measurement of low ion currents and the instrument stability required for long measurement times. The natural abundance of the clumped molecules is very low i.e., about $4.9*10^{-6}$ and $7.8*10^{-8}$ of the total CH_4, for $^{13}CH_3D$ and $^{12}CH_2D_2$, respectively. The corresponding ion currents are proportionally low, typically around 6000 cps for $^{13}CH_3D^+$ and 100 cps for $^{12}CH_2D_2^+$. The cumulated number of counts control the limits of the achievable precision for the rare isotopologues. Therefore, to achieve permil-level precision, the isotopologue ratios need to be measured for a long time. This requires several mL (1mL (STP) = ~45 μmol) of pure CH_4 for one measurement. To obtain pure-CH_4 for the measurements, the samples need to be purified. Isotope fractionation can occur during sample handling, extraction, and purification, potentially introducing biases and inaccuracies in the measured bulk and clumped isotopologue ratios. Careful consideration of sample preparation methods, including minimizing fractionation and optimizing purification procedures, is crucial to ensure reliable and reproducible results. Another hurdle is that there are no readily available reference gases with known clumped isotopic composition to calibrate the measurements, so these need to be prepared.

A number of studies have reported the $\Delta^{13}CDH_3$ and $\Delta^{12}CD_2H_2$ of CH_4 from various sources, e.g. natural gas seeps, rice paddies and wetlands, lake sediments, shale gas, coal mines, natural gas leakage, laboratory incubation experiments (Wang et al., 2015; Young et al., 2017; Stolper et al., 2018; Loyd et al., 2016; Ono et al., 2021; Giunta et al., 2019). A general overview of the expected clumped isotope signatures of CH_4 from different sources is illustrated in Fig 1b. Thermogenic CH_4 is usually formed in thermodynamic equilibrium and therefore lies on the thermodynamic equilibrium curve between 100-300 °C. Biogenic CH_4 production, denoted as methanogenesis in Fig 1b, is often characterised by dis-equilibrium $\Delta^{12}CD_2H_2$ values due to the kinetic isotopic fractionation associated with methanogenesis and/or combinatorial effects (Röckmann et al., 2016a; Yeung, 2016). The reported range of values for abiotic (produced at high and low temperatures) and pyrogenic CH_4 is also shown in Fig 1b. The predicted clumping anomaly of the atmospheric CH_4 source mix resulting from the combination of all sources is about 4 ‰ for $\Delta^{13}CDH_3$ and 20 ‰ for $\Delta^{12}CD_2H_2$, as reported by Haghnegahdar et al. (2017) (Fig 1b).

Recent modelling studies have suggested the potential of clumped isotope measurements of atmospheric CH_4, especially $\Delta^{12}CD_2H_2$, to distinguish between the main drivers of change in the CH_4 burden (Chung and Arnold, 2021; Haghnegahdar et al., 2017). However, as mentioned above, the clumped isotope measurements require a few mL (at STP) of pure CH_4. Therefore, a challenge specific to atmospheric CH_4 measurements is the extraction of CH_4 from very large samples of air required (thousands of litres).

This paper presents one of the first measurements of the clumping anomalies of atmospheric methane and provide a detail comparison to the previously reported model predictions. The paper also describes in detail the technical setups and procedures for CH_4 clumped

measurements at Utrecht University including (i) the extraction and purification of CH_4 from high and low concentration samples, including the extraction from large quantities of air (~ 1000 L); (ii) calibration of measured anomalies using gas-equilibration experiments at different temperatures; (iii) the detailed settings and procedures of the actual isotope measurements using the Thermo Ultra mass spectrometer and (iv) the data processing and calculations involved. We also report the performance of these systems so far, in terms of precision, reproducibility, stability, etc. Thus, this paper serves as description of our measurement technique for future reference.

2. Methods

2.1 Notations, definitions, and calculations

The bulk isotopic composition of CH_4, denoted as $\delta^{13}C$ and δD, is defined as follows:

$$\delta^{13}C_{sample} = \frac{R^{13C}_{sample}}{R^{13C}_{VPDB}} - 1 \qquad \textit{(Equation 1a)}$$

$$\delta D_{sample} = \frac{R^{D}_{sample}}{R^{D}_{VSMOW}} - 1 \qquad \textit{(Equation 1b)}$$

where, R^{13C}_{sample} and R^{D}_{sample} are the isotopic ratios of $^{13}C/^{12}C$ and D/H of the sample and R^{13C}_{VPDB} and R^{D}_{VSMOW} are isotopic ratios of the international standards for $\delta^{13}C$ and δD (VPDB and VSMOW) and their values are 0.011180 and 0.00015576 respectively (Assonov et al., 2020; Gonfiantini, 1978).

The clumped isotopic composition of CH_4 is expressed as clumping anomalies $\Delta^{13}CDH_3$ and $\Delta^{12}CD_2H_2$ relative to the clumped isotope ratio that would be obtained if the heavy isotopes ^{13}C and D were distributed randomly across all isotopologues in the same sample:

$$\Delta^{13}CDH_{3\,sample} = \frac{R^{13CD}_{sample}}{(4 * R^{13C}_{sample} * R^{D}_{sample})} - 1 \qquad \textit{(Equation 2a)}$$

$$\Delta^{12}CD_2H_{2\,sample} = \frac{R^{DD}_{sample}}{(6 * (R^{D}_{sample})^2)} - 1 \qquad \textit{(Equation 2b)}$$

R^{13CD}_{sample} and R^{DD}_{sample} are the isotopologue ratios of $^{13}CDH_3/^{12}CH_4$ and $^{12}CD_2H_2/^{12}CH_4$ of the sample and R^{13C}_{sample} and R^{D}_{sample} are isotope ratios of $^{13}C/^{12}C$ and D/H of the sample itself. The denominator in the Equations 2a and 2b give the expected random distribution of the heavier isotopes in a sample, where 4 and 6 are symmetry factors (Young et al., 2017).

2.2 Mass spectrometer specifications and measurement methods

CH_4 bulk and clumped isotopic compositions are determined using the Thermo Scientific Ultra HR-IRMS. The prototype of the instrument was introduced by Eiler et al. (2013) and the characteristics of the Thermo Ultra at Utrecht University have been explained in detail by Adnew et al. (2019). The instrument is operated with the advanced Qtegra™ software package, for data acquisition, instrument control, and data analysis.

The sample is introduced via one of the four variable volume bellows into the ion source and reference gas is provided from another bellow. After ionization in the ion source, the ion beam is accelerated, focused, and passed through a slit into the mass analyzer. Three different slit widths of 250,16, and 5 μm can be chosen in the standard setup, giving three resolution options: low (LR), medium (MR) and high resolution (HR), respectively. An additional 'aperture' option can be turned on to achieve even higher resolution (HR+), wherein the focused ion beam is trimmed further in the Y axis by an additional slit situated just before the electromagnet. However, increasing the resolution results in a decrease of intensity.

The ions are separated by energy and mass in the mass analyzer, which leads to very well focussed ion beams, and they are collected with a variable detector array that supports one fixed and eight moveable detector platforms, which are equipped with nine Faraday detectors (L1, L2, L3, L4, Center, H1, H2, H3, H4) that can be read out with selectable resistors with resistances between $3 \times 10^8\ \Omega$ and $10^{13}\ \Omega$. The three collector platforms at the high mass end (H2, H3 and H4) are additionally equipped with compact discrete dynode (CDD) ion counting detectors next to the Faraday detectors.

2.2.1 Characterization of the Ultra for CH_4 measurements

Clumped isotope measurements of CH_4 using the Ultra are performed at high resolution (5 μm entrance slit width) with aperture i.e., HR+ setting, to get the highest possible resolution. Two Faraday collectors are read out with resistors, $1 \times 10^{11}\ \Omega$ for *m/z* 16 and $1 \times 10^{12}\ \Omega$ for *m/z* 17-$^{13}CH_4$. To measure m/z 17-$^{12}CDH_3$ and the clumped isotopologues at m/z 18, we use the CDD of detector H4, which has a narrow detector slit. With careful tuning, the instrument can achieve mass resolving power (5-95%) higher than 42,000, which is sufficient to separate CH_4 isotopologues from each other, from contaminating isobars like H_2O^+, OH^+ and NH_3^+, and the adducts formed in the source, $^{12}CH_5^+$, $^{13}CH_5^+$ and $^{12}CDH_4^+$.

As the high resolution is to a large degree achieved by using a very narrow source slit, most of the ions do not pass through the slit but deposit on the slit assembly. This leads to carbon accumulation around the slit and over time obstructs the passage of ions into the mass analyzer, resulting in reduced ion transmission and sensitivity. The carbon deposits can also introduce additional scattering and deflection of ions, leading to the broadening of mass peaks and decreased mass resolution. There can also be signal instabilities due to fluctuations

in ion transmission. These effects together can compromise the instrument's capability to resolve closely spaced ions. Therefore, we change the source slit regularly to avoid the impact of carbon deposits. To keep track of this, the number of counts of $^{12}CH_4^+$ of each measurement is monitored (Fig S1 in supplement). When the counts decrease to less than 0.5 times the counts of the first measurement using a new slit, the slit is replaced. The usual lifetime of one slit is around 6 months, depending on the number of CH_4 measurements done.

The main CH_4 isotopologues, $^{12}CH_4^+$, $^{13}CH_4^+$, $^{12}CH_3D^+$, $^{13}CH_3D^+$, and $^{12}CH_2D_2^+$ are measured in three different configurations on the Ultra. The configurations differ by the peak center mass setting and the relative distance between the detectors and the peak positions are finely adjusted (Fig 3) such that the right ions are detected by each detector. The details of the three different configurations, resistors and detectors used for the measurements on the Ultra are given in Table 1. In the first configuration, $^{12}CH_4^+$ (L1) and $^{12}CH_3D^+$ (H4-CDD) are measured for about 3 hours. The second configuration is set up to measure $^{12}CH_4^+$ (L3), $^{13}CH_4^+$ (L1), and $^{13}CH_3D^+$ (H4-CDD) and the third configuration to measure $^{12}CH_4^+$(L3), $^{13}CH_4^+$ (L1), and $^{12}CH_2D_2^+$ (H4-CDD). Configurations 2 and 3 are measured alternately for 18 hours in 7 cycles each lasting about 2.5 hours. Therefore, in total, one complete measurement of all three configurations takes about 20 hours. The sample and reference gases are measured alternately, each three times (= integrations) for a total of 201.3 seconds; the average of which is considered one data point. The result of one complete measurement is the average of all the data measured (outliers removed) and the internal precision is the standard error over these data points.

A summary of the natural abundances, molecular masses, expected intensity in cps (for AP613, the laboratory reference gas), and the counting statistics precision limit for all the five isotopologues are given in Table 2.

Table 1: The details of the three different configurations, resistors and detectors used for the measurements on the Ultra.

Configuration	**L3 width: 1.3 mm** (amplifier)	**L1 width: 0.6 mm** (amplifier)	**H4-CDD width: 0.04 mm**	**Center mass (Latest mass calibration) (amu)**	**Measurement times (h)**
1:δD		$^{12}CH_4^+$ (10^{11} Ω)	$^{12}CH_3D^+$	17.2612	3
2:$\delta^{13}C$, $\Delta^{13}CDH_3$	$^{12}CH_4^+$ (10^{11} Ω)	$^{13}CH_4^+$ (10^{12} Ω)	$^{13}CH_3D^+$	18.4799	9
3: $\Delta^{12}CD_2H_2$	$^{12}CH_4^+$ (10^{11} Ω)	$^{13}CH_4^+$ (10^{12} Ω)	$^{12}CH_2D_2^+$	18.4825	9

Table 2: A summary of the natural abundances, molecular masses, expected intensity in cps (for AP613, the laboratory reference gas), and the counting statistics precision limit for an integration time of 201.3 seconds for all the five isotopologues of CH_4 measured on the Ultra.

Isotopologue	Natural abundance (%)	Molecular mass	Intensity in cps (AP613)	Counting statistics (‰)
$^{12}CH_4$	98.88	16.0313	$9*10^{8}$	$2.3*10^{-03}$
$^{13}CH_4$	1.07	17.034	$9.5*10^{6}$	0.023
$^{12}CDH_3$	0.045	17.0376	$5*10^{5}$	0.099
$^{13}CDH_3$	$4.9*10^{-04}$	18.0409	5000	0.99
$^{12}CD_2H_2$	$7.8*10^{-06}$	18.0439	90	7.43

The gasses are measured at a source pressure of maximum $2.5*10^{-7}$ mbar. The pressure in the source is controlled by the bellow pressure, which can be set and adjusted using Qtegra. The typical pressure in the bellows required to achieve this source pressure for CH_4 is around 65-70 mbar. We use a continuous pressure adjustment method, which is, after each integration, the bellow pressures are checked 5 times, and the bellows are compressed by 0.5 % each time, until the set value is attained. The tolerance of the pressure adjustment is set to 0.5 mbar, so that the signal is stable within ± 0.7 %. This ensures that the instrument measures the reference and sample at the same source pressure during the entire 20+ hours of measurement time.

All measurements are made relative to a reference gas, which is a stainless-steel canister filled from a high purity (>99.999%) CH_4 reference gas cylinder (AP613). The sample and the reference are measured alternately, and then the bulk and clumped isotopic composition of the samples are calculated from the isotopologue ratios as follows:

$$\delta^{13C}_{sam-VPDB} = \delta^{13C}_{sam-ref} + \delta^{13C}_{ref-VPDB} + (\delta^{13C}_{sam-ref} * \delta^{13C}_{ref-VPDB}) \qquad \textit{(Equation 3a)}$$

$$\delta^{D}_{sam-VSMOW} = \delta^{D}_{sam-ref} + \delta^{D}_{ref-VPDB} + \left(\delta^{D}_{sam-ref} * \delta^{D}_{ref-VSMOW}\right) \qquad \textit{(Equation 3b)}$$

$$\Delta^{13CDH_3}_{sam} = \frac{\left(1+\delta^{13CDH_3}_{sam-ref}\right)*\left(1+\Delta^{13CDH_3}_{ref}\right)}{\left(1+\delta^{13C}_{sam-ref}\right)*\left(1+\delta^{D}_{sam-ref}\right)} - 1 \qquad \textit{(Equation 3c)}$$

$$\Delta^{12CD_2H_2}_{sam} = \frac{\left(1+\delta^{12CD_2H_2}_{sam-ref}\right)*\left(1+\Delta^{12CD_2H_2}_{ref}\right)}{\left(1+\delta^{D}_{sam-ref}\right)^{2}} - 1 \qquad \textit{(Equation 3d)}$$

$\delta^{13C}_{sam-ref}$, $\delta^{D}_{sam-ref}$, $\delta^{13CDH_3}_{sam-ref}$ and $\delta^{12CD_2H_2}_{sam-ref}$ are the values of the sample measured against the reference calculated from the measured ion intensities on the Ultra. These values are

converted to the standard scales: $\delta^{13C}_{sam-VPDB}$, $\delta^{D}_{sam-VSMOW}$, $\Delta^{13_{CDH_3}}_{sam}$ and $\Delta^{12_{CD_2H_2}}_{sam}$ using the formulae above. The clumping anomalies of the reference gas used for the measurements, AP613, denoted as $\Delta^{13_{CDH_3}}_{ref}$ and $\Delta^{12_{CD_2H_2}}_{ref}$, were assigned using temperature-equilibration experiments which are explained in detail in the next section. The bulk isotopic composition of AP613 denoted as $\delta^{13C}_{ref-VPDB}$ and $\delta^{D}_{ref-VSMOW}$, was obtained by measurements using a conventional continuous flow IRMS system (Menoud et al., 2021).

2.3 Temperature calibration scale

To produce a CH_4-clumped isotope calibration scale, we performed a series of isotope exchange experiments at various temperatures. For this, the laboratory reference gas, AP613 was used, which is a commercially available pure CH_4 cylinder with known bulk isotopic composition. CH_4 from AP613 was equilibrated at temperatures ranging from 50 to 450 °C using two different catalysts: γ-Al_2O_3 for temperatures below 200 °C and Pt on Al_2O_3 for 200-450 °C.

Both catalysts were activated using the procedure explained in Eldridge et al. (2019). For each heating experiment, about 10 pellets of the catalyst were inserted in a 20 mL glass tube with a Teflon valve and evacuated to 10^{-3} mbar to remove adsorbed air and moisture. The tube was then filled with 140 mbar of pure O_2 and heated for about 5 hours at 550 °C for activation of the catalyst. After heating, the tube was evacuated overnight (12-14 hours) at 550 °C and then cooled to room temperature. The pellets were not exposed to outside air once activated. After the activated pellets were cooled to room temperature, 5-6 mL of pure CH_4 (AP613) was added to the tube and heated at the desired temperature and duration as given in Table 3.

The equilibrated gases were measured on the Ultra against the reference gas, i.e., unmodified CH_4 from the AP613 cylinder. The raw $\Delta^{13}CDH_3$ and $\Delta^{12}CD_2H_2$ values are calculated using equations 3c and 3d but assuming $\Delta^{13_{CDH_3}}_{ref}$ and $\Delta^{12_{CD_2H_2}}_{ref}$ to be zero. The raw values obtained in this way showed the expected dependence on temperature but with a shift due to the real clumped values of the reference being different from zero. To determine this offset, the functions from Eldridge et al. (2019) were fit to the data with an added free parameter for the offset as given in equations 4a and 4b:

$$\Delta^{13}CDH_3 = a + \frac{1.47348\,x\,10^{19}}{T^7} - \frac{2.08648\,x\,10^{17}}{T^6} + \frac{1.1981\,x\,10^{17}}{T^5} - \frac{3.54757\,x\,10^{12}}{T^4} + \frac{5.54476\,x\,10^{9}}{T^3} - \frac{3.49294\,x\,10^{6}}{T^2} + \frac{8.8937\,x\,10^{2}}{T} \quad \textit{(Equation 4a)}$$

$$\Delta^{12}CD_2H_2 = b - \frac{9.67634\,x\,10^{15}}{T^6} + \frac{1.71917\,x\,10^{14}}{T^5} - \frac{1.24819\,x\,10^{12}}{T^4} + \frac{4.30283\,x\,10^{9}}{T^3} - \frac{4.4866\,x\,10^{6}}{T^2} + \frac{1.86258\,x\,10^{3}}{T} \quad \textit{(Equation 4b)}$$

The parameters *a* and *b* were then optimized, keeping the shape of the temperature dependence constant, and were used to estimate the $\Delta^{13}CDH_3$ and $\Delta^{12}CD_2H_2$ values of our reference gas. In practice, this was done using a Monte Carlo simulation with 1000 runs: at each run, each data point was independently applied a random error based on the uncertainty of that measurement, assuming Gaussian distribution of the errors. The functions above were then fitted, and a set of free parameters (*a* and *b*) were obtained. The final absolute $\Delta^{13}CDH_3$ and $\Delta^{12}CD_2H_2$ values of the reference were calculated by averaging the *a* and *b* parameters for all runs (with outliers removed) and the errors reported are the corresponding standard deviations.

2.4 CH_4 extraction and purification system

The schematic of the extraction system is shown in Fig 2:

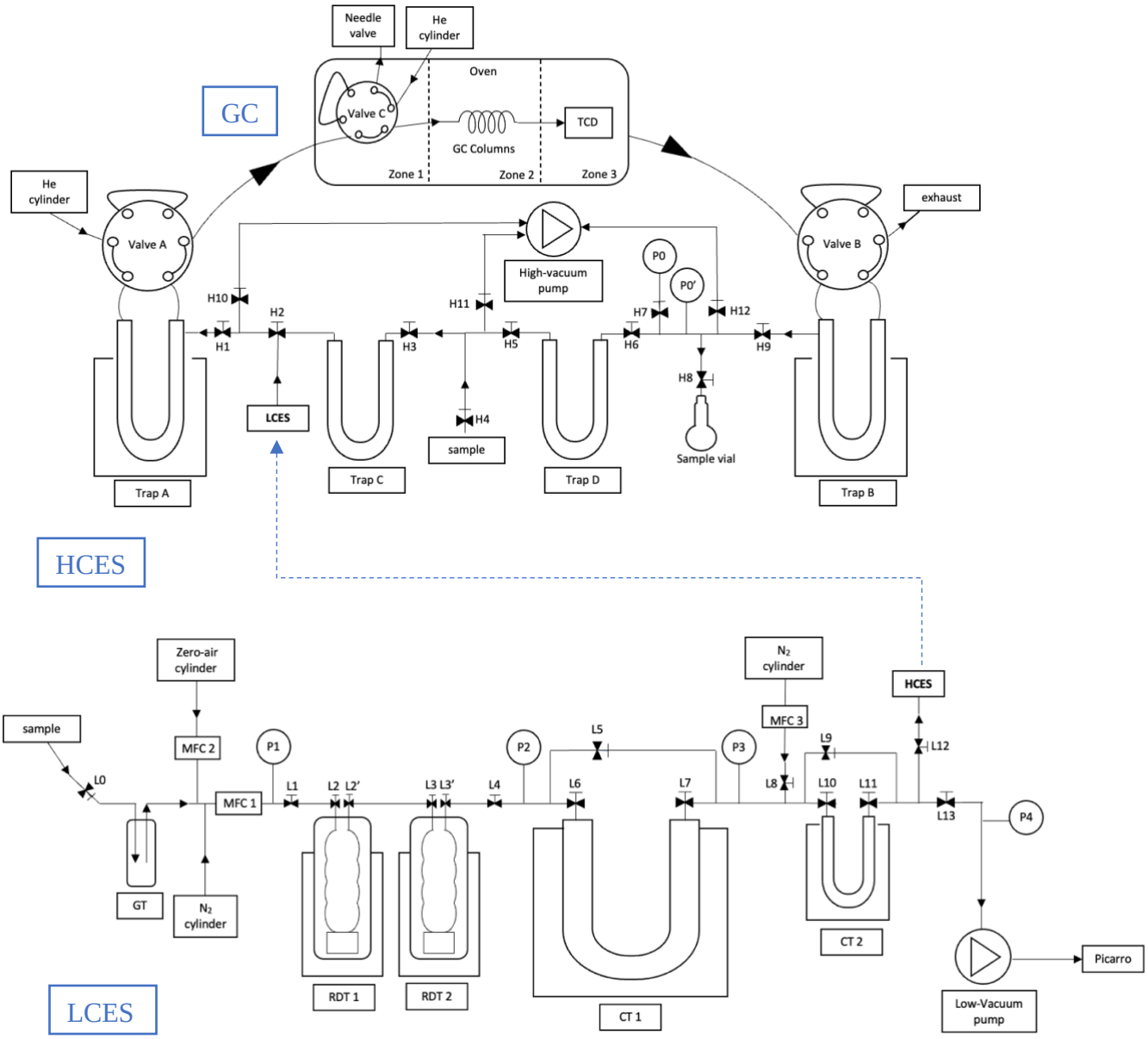

Fig 2: Schematic of high-concentration (HCES) and low-concentration (LCES) extraction system and the GC setup at IMAU. Samples are introduced to the HCES via H4 and to the LCES via L0. The pre-concentrated sample in CT2 is transferred to Trap A via a connection between L12 and H2. The acronyms used in the figures are explained in the main text (Section 2.4)

Precise measurements of the clumped isotopic composition of CH_4 on the Ultra requires about 3 ± 1 mL of pure CH_4 for a single measurement. Throughout this paper the quantity of gas is specified in mL (at STP unless otherwise specified; the conversion to molar units is: 1 mL = ~45 μmol).

The CH_4 extraction and preconcentration procedure followed in our laboratory involves several steps depending on the sample concentration as explained below.

2.4.1 HCES

The high-concentration extraction system (HCES) is used to extract CH_4 from samples with more than 1 % of CH_4 i.e., extracting from up to 200 mL of sample gas. The HCES includes two empty traps (Trap C and Trap D), two traps filled with silica gel (Trap A and Trap B), and a gas chromatograph (GC) with a passive Thermal Conductivity Detector (TCD), all connected with ¼'' SS tubing and 316L VIM-VAR Swagelok valves. All the parts are shown in the schematic above (Fig 2). This system is built following the one described in Young et al. (2017).

The CH_4 in the sample gas is separated from the other components by GC, and then collected cryogenically on silica gel. The sample is introduced via valve H4 and collected in Trap A with silica gel cooled to -196 °C with liquid N_2. The pressure in the system is monitored to ensure that all the sample is trapped. The sample in Trap A is introduced into the GC from Trap A using He at a flow rate of 30 mL/min for 5 min by warming the trap to about 70 °C using a hot water bath.

The GC has two columns used in series for the final purification of CH_4. A 5-meter ¼'' OD SS column packed with 5Å molecular sieve to separate H_2, Ar, O_2 and N_2 from hydrocarbons and a 2-meter ¼'' OD SS column packed with HayeSep D porous polymer to separate CH_4 from the remaining higher hydrocarbons like C_2H_6, C_3H_8, etc. Wide columns of ¼'' are used to attain separation of more than 5 mL of CH_4 within 55 min.

CH_4 elutes from the GC column after O_2, N_2, and Kr. For concentrated samples (>5 % CH_4 in air) without Kr, O_2 elutes around 10 min, N_2 around 22 min and CH_4 around 40 min when the GC is operated at 50 °C. After the complete elution of N_2 (35 min), Trap B with silica gel is cooled with liquid N_2 to collect CH_4 for about 15 min. Once all the CH_4 is collected, Trap B is evacuated for 10 min to remove the He carrier gas while the trap is still cooled with liquid N_2.

Following this, CH_4 is released from the Trap B by warming the trap to ~ 70 °C (hot water bath) and collected in a sample vial filled with Silica gel and cooled with liquid N_2 to be transferred to the mass spectrometer.

For samples with CH_4 concentrations between 1 % and 5 % CH_4 in air, the sample volumes required to extract the required amount of CH_4 are larger (>100 mL). In this case, the O_2 and N_2 peaks are not fully resolved, and not well separated from CH_4. Therefore, CH_4 along with traces of O_2 and N_2 eluted from the GC is collected in Trap A instead of the sample vial and passed through the GC a second time for further purification (same steps as above). In the second round of extraction, the O_2 and N_2 peaks are small and well separated from each other and from the CH_4 peak. For samples with ppm levels of Kr (notably atmospheric samples), separation of pure CH_4 from Kr was only achieved when the GC columns were heated at 40 °C instead of 50 °C normally used for other samples. The comparison of chromatograms before and after Kr separation was achieved is shown in Fig 9.

After each chromatographic separation, the GC columns are baked at 200 °C for 30 min with He flow to remove CO_2, the heavier hydrocarbons, and other impurities. After baking, the columns are slowly cooled to 50 °C for the next extraction. Traps A and B are heated overnight at 150 °C while pumping with a high vacuum pump. The silica gel flask used for sample collection is evacuated until the next use.

2.4.2 LCES

Extracting CH_4 from large quantities of air involves a stepwise increase of the CH_4 concentration by cryogenically trapping the sample gas in successively smaller charcoal traps, until the concentration is high enough for the sample to be further processed with the HCES. The low-concentration extraction system (LCES) is made of a 1/2" glass tube with J. Young high-vacuum PTFE valves and the major components are an empty glass trap (GT), two Russian Doll Traps (RDT1 and RDT2), and two charcoal traps (CT1 and CT2) as shown in Fig 2. A part of LCES is from the extraction system that has been used previously for CO isotope analysis (Bergamaschi et al., 2000; Bergamaschi et al., 1998).

The GT and RDTs are respectively used to remove H_2O and CO_2 from the air. This is followed by two pre-concentration steps in CT1 and CT2, which both collects all the CH_4 but only a small part of bulk air so that the CH_4 concentration increases in each step. The exhaust of the low-vacuum pump which draws the air though the extraction system is connected to a G2301 greenhouse gas analyzer (Picarro Inc.) to monitor CO_2, CH_4, and H_2O concentrations during the whole extraction procedure. This ensures that a potential breakthrough is detected.

The air taken directly from outside or from a cylinder is first dried using GT cooled to -70 °C with a dry ice - ethanol slurry. A $Mg(ClO_4)_2$ tube after GT further dries the air sample before it is introduced to the traps for collection. RDT1 and RDT2, both cooled to -196 °C with LN_2 and connected in series, are used to scrub CO_2, N_2O, H_2O traces and other condensable gases from the air. The CO_2-free air is then passed through CT1 (-196 °C) which traps CH_4

quantitatively, and only part of the remaining air components (O_2, N_2, etc). During this CT1 collection period, CT2 is bypassed. The flow of air is controlled using a Mass Flow Controller (MFC 1) and is adjusted to 6-6.5 L/min to maintain a pressure lower than 230 mbar in the glass line between L1 and L6 to avoid condensation of O_2 in the traps cooled with liquid N_2, which is a potential danger. The glass line is partially heated using heating wires to avoid freezing of tubes and valves.

Once a quantity of about 1100 L of air has been processed, the remaining air in the glass line is pumped until P4 drops to 4 mbar. To transfer the collected air from CT1 to CT2, the liquid N_2 around CT1 is replaced with dry ice + EtOH slurry to warm the trap to -70 °C. At this temperature, the emerging N_2 + O_2 mixture is pumped out for 3-4 min, while the CH_4 stays in the CT1 trap. In the meantime, the bypassed CT2 is cooled to -196 °C with LN_2. The remaining gas mix in CT1 is released by removing the dry ice slurry and heating CT1 with a hot water bath and is passed through CT2 (-196°C). As the pressure in the line drops to 10 mbar, 0.5 L/min of additional pure N_2 is used to transfer any remaining gas from CT1 to CT2 for 5 min via MFC 1. After this, the liquid N_2 bath of CT2 is replaced with dry ice + EtOH slurry and pumped for 1-2 min to further concentrate the air mixture. At the end of this step, the final sample volume is less than 100 mL, and the sample can be transferred to Trap A of the HCES cooled with liquid N_2. CT2 is heated using a water bath and, after the pressure reading on P3 drops to 0 mbar, it is flushed with pure N_2 from MFC 3 (at 5 mL/min for 2 min) to transfer the remaining gas. Once all the sample is collected in Trap A, the high-concentration extraction procedure is followed as explained above.

For samples with medium concentrations (0.1-1 % CH_4) i.e., < 3 L total sample volume, the first few steps of LCES are skipped and the sample is directly trapped in CT2. The remaining procedure is the same as explained above.

Before each extraction, RDTs and CTs are cleaned using 0.5 L/min of pure N_2 for 40 min while heating them with hot water baths at 70 °C to avoid contamination from the previous sample.

2.4.4 Extraction system tests with laboratory reference gas

The extraction and purification system was tested using three of our laboratory reference gases: AP613, CAL1549 and IMAU-3. Various mixtures of pure-AP613 in zero air (synthetic air, O_2+N_2) and pure-CAL1549 in zero air were used to test the extraction system, and then the extracted CH_4 was measured on the Ultra. The separation of Kr from CH_4 in the GC and the effect on Kr on the isotope measurements on the Ultra were tested using a 1:1 mixture of IMAU-3 and pure Kr.

To replicate the atmospheric CH_4 samples, pure-AP613 was mixed with zero air to a mole fraction of 2.5 ppm of methane in 1000 L. Since zero air is devoid of CO_2 and H_2O, GT and RDT2 were bypassed for these tests. RDT1 was still immersed in LN_2 to ensure that even

small traces of CO_2 were trapped and to check that the RDTs do not influence the clumping anomalies of CH_4. The rest of the procedure was followed as for normal sampling.

2.5 Quality checks for the Thermo Ultra

To establish the accuracy of the Ultra measurements, the Ultra δD and $\delta^{13}C$ measurements are compared to conventional bulk isotope measurements. Most samples are analysed for δD and $\delta^{13}C$ before the extraction and purification, using an independent conventional bulk isotope measurement system (Menoud et al., 2020), and the results are compared to the ones obtained from the Ultra measurements after the extraction.

Weekly "zero enrichment" measurements (same gas in both bellows) are done to check for systematic difference between the bellows (e.g., by contamination, leaks, etc). These, together with regular measurements of the pure CAL1549 gas, are used to monitor the stability of the instrument and the reproducibility of the measurements. The internal precision of the measurements is estimated for each measurement (sample or test gas) from the 1se (standard error) over the whole measurement.

An inter-laboratory comparison with the the Nu Panorama high-resolution mass spectrometer operated at University of Maryland (UMD) was done for the three laboratory reference gases: AP613, CAL1549 and IMAU-3. The results of these comparisons are presented in the next section.

3. Results and Discussion

3.1 Thermo Ultra measurements

As described in section 2.2, clumped isotope measurements on the Ultra involve measuring the different isotopologues in three configurations for a total of 20 hours. Typical mass scans of the three configurations are shown in Fig 3. The position of the peak centers (marked with red dotted lines in Fig 3) is quite stable during the entire measurement procedure and small mass shifts are corrected every hour using the peak center correction feature in the software.

Configuration 1: $^{12}CH_4$ and $^{12}CDH_3$

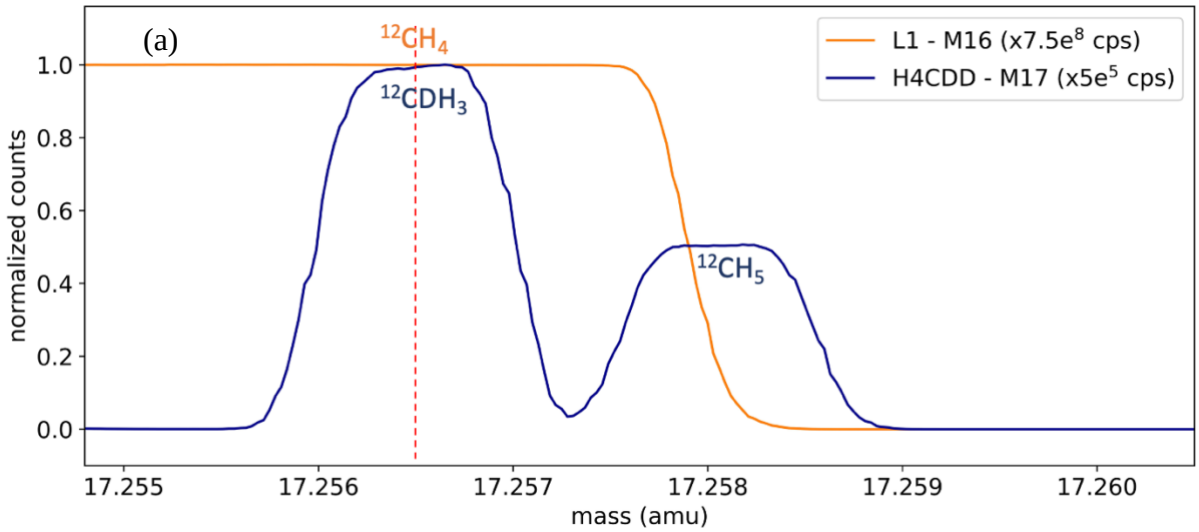

525
526
527

Configuration 2: $^{12}CH_4$, $^{13}CH_4$ and $^{13}CDH_3$

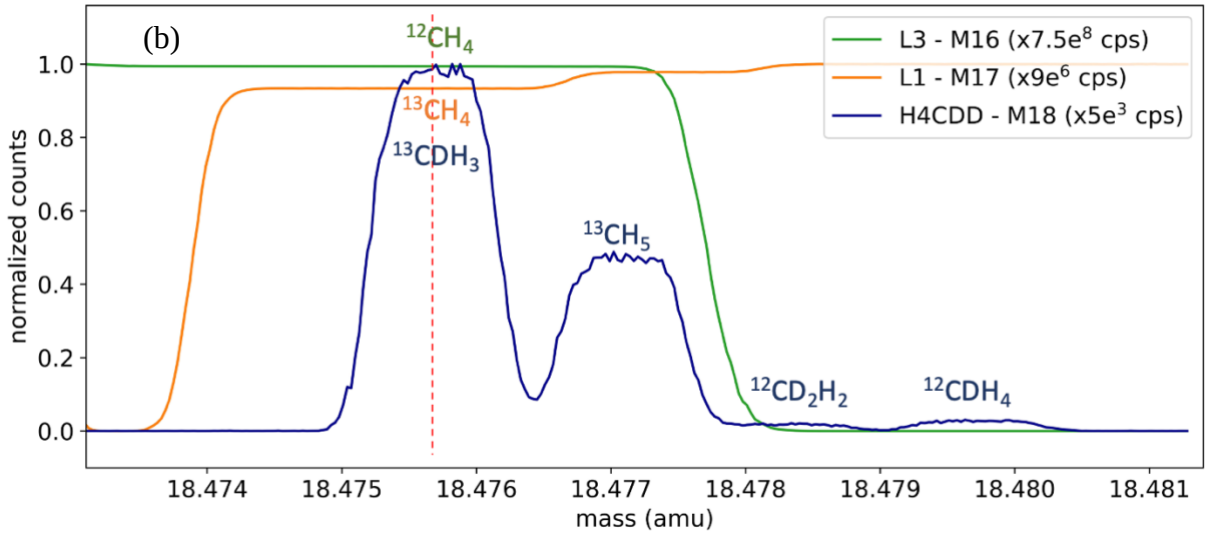

528
529
530

Configuration 3: $^{12}CH_4$, $^{13}CH_4$ and $^{12}CD_2H_2$

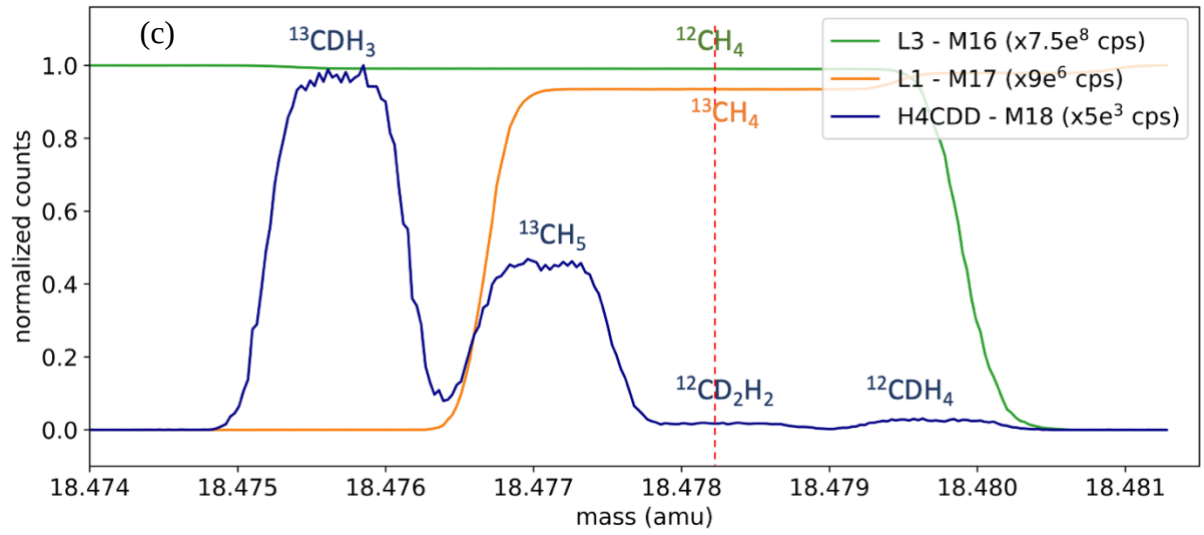

531
532

Zoomed $^{12}CD_2H_2$ peak.

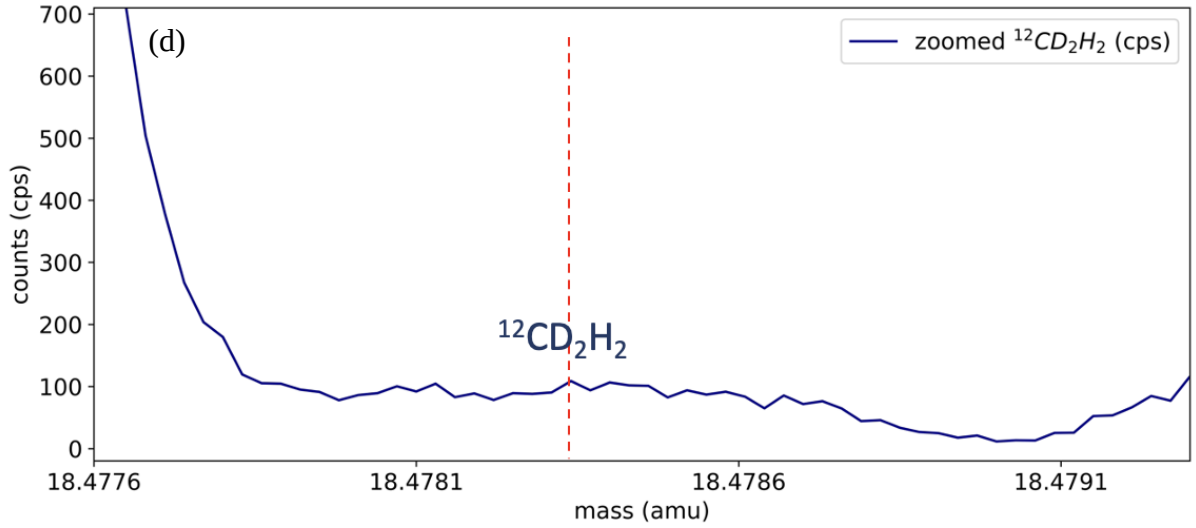

Fig 3: Mass scans of three configurations to measure $^{12}CDH_3$ (a), $^{13}CH_4$ and $^{13}CDH_3$ (b), $^{13}CH_4$ and $^{12}CD_2H_2$ (c and d). The x-axis values correspond to the peak center setting i.e., mass-17 in (a) and mass-18 in (b-d) and the other detectors are offset to these values to show the other isotopologues on the same scale. The different detectors used, and the normalization factors are given in the legends. The red dashed line indicates the peak center mass setting. (d) shows the zoomed peak of $^{12}CD_2H_2$ and the counts measured.

3.2 Temperature equilibration experiments

The results of the heating experiments are presented in Table 3. The equilibrated gas (subsample of AP613 heated at different temperatures (section 2.3)) was measured against the non-equilibrated gas from AP613 (directly from the cyclinder), which is the Ultra reference gas. Raw measurement values relative to the reference gas are reported as $\Delta^{13}CDH_3$ raw and $\Delta^{12}CD_2H_2$ raw.

Table 3: Summary of the equilibrated gas experiments, $\Delta^{13}CDH_3$ raw and $\Delta^{12}CD_2H_2$ raw values are relative to the reference gas and $\Delta^{13}CDH_3$ absolute and $\Delta^{12}CD_2H_2$ absolute are calculated using the assigned anomalies of the reference gas.

Temp (°C)	Catalyst	Duration (h)	$\Delta^{13}CDH_3$ (raw) (‰)	$\Delta^{13}CDH_3$ (absolute) (‰)	se	$\Delta^{12}CD_2H_2$ (raw) (‰)	$\Delta^{12}CD_2H_2$ (absolute) (‰)	se
50	γ-Al_2O_3	624	3.17	5.44	0.4	10.73	13.49	1.7
150	γ- Al_2O_3	66	0.86	3.13	0.3	4.81	7.56	2.3
250	Pt/ Al_2O_3	120	-0.31	1.95	0.3	4.02	6.77	2.6
300	Pt/ Al_2O_3	64	-0.69	1.57	0.3	0.97	3.71	2.0
350	Pt/ Al_2O_3	144	-0.64	1.62	0.3	-2.44	0.29	2.4
400	Pt/ Al_2O_3	108	-1.14	1.12	0.2	-0.08	2.66	1.6

The measured values of heated AP613 at different temperatures were compared to the theoretical equilibrium curve, and the $\Delta^{13}CDH_3$ and $\Delta^{12}CD_2H_2$ values of AP613 were estimated using the Monte Carlo simulations as described in Sect. 2.3. The $\Delta^{13}CDH_3$ and $\Delta^{12}CD_2H_2$ assigned to our reference gas, AP613 are: $\Delta^{13}CDH_3 = 2.23 \pm 0.12$ ‰ and $\Delta^{12}CD_2H_2 = 3.1 \pm 0.9$ ‰. Since this pair of values for the clumping anomalies doesn't lie on the thermodynamic equilibrium curve, we cannot assign a formation temperature value to AP613. The absolute values of $\Delta^{13}CDH_3$ and $\Delta^{12}CD_2H_2$ calculated using the assigned values of AP613 are given in Table 3 and in Fig 4.

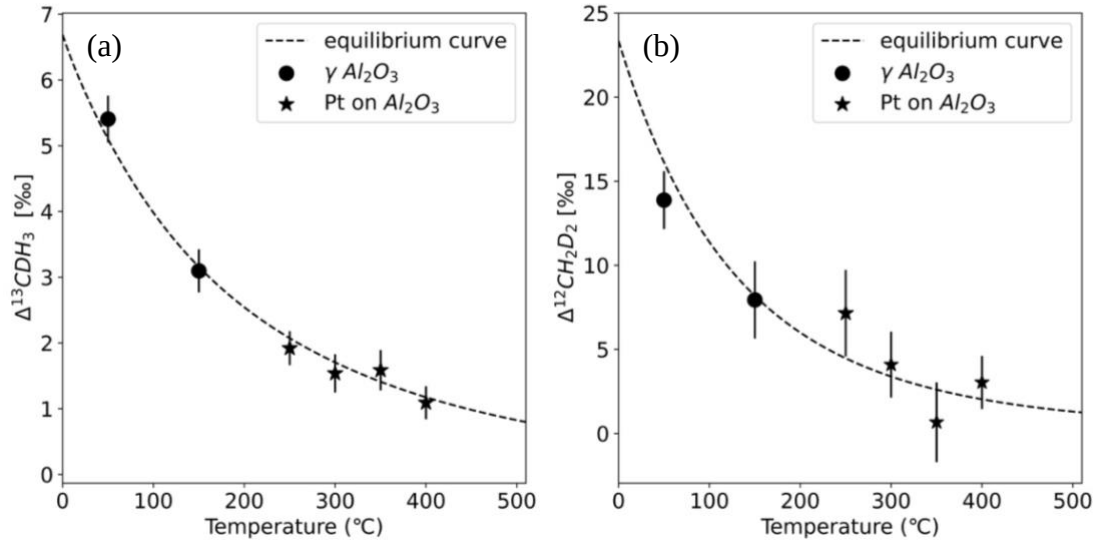

Fig 4: Absolute $\Delta^{13}CDH_3$ and $\Delta^{12}CD_2H_2$ of the equilibrated gas compared to the theoretical equilibrium curve, calculated using the assigned anomalies of the reference gas, AP613: $\Delta^{13}CDH_3 = 2.23 \pm 0.12$ ‰ and $\Delta^{12}CD_2H_2 = 3.1 \pm 0.9$ ‰. The data points represent the equilibrated gas at different temperatures with the markers corresponding to the different catalysts as given in the legend. The black dashed line is the thermodynamic equilibrium curve.

3.3 Internal precision and reproducibility of the Ultra measurements

The average standard error of the measured $\delta^{13}C$, δD, $\delta^{13}CDH_3$ and $\delta^{12}CD_2H_2$ values and its comparison to the expected precision based on counting statistics of the shot noise are given in Table 4. Achieved precisions are very close to the shot noise limit for $\delta^{13}C$, $\delta^{13}CDH_3$ and $\delta^{12}CD_2H_2$. Typically, δD measurements are about 2 times worse than the shot noise limit. This may be because of the following reasons: The high-count rates (order of 10^5) of $^{12}CH_3D$ measured using the H4-CDD detector, are close to the upper limit of the CDD operating range, and not in the optimal region. Therefore, we expect here a lower signal-to-noise ratio (= a higher relative error). Additionally, the peak top of $^{12}CH_3D$, which is not very flat and sometimes rounded, suggest that the ion beam is slightly too wide for H4-CDD with a very narrow collector slit, which is not unexpected given the relatively high abundance. That means, very slight variations in the ion beam direction can result in relatively large variations in the quantity of ions entering the detector. However, the changes in δD between different samples are much higher than the achieved precision, which is better than the one for conventional CF-IRMS instruments.

The average precision (1 se (standard error)) of calculated clumping anomalies of over 300 measurements in the last 3 years, is 0.3 ± 0.1 ‰ for $\Delta^{13}CDH_3$ and 2.4 ± 0.8 ‰ for $\Delta^{12}CD_2H_2$ depending on the CH_4 sample volume and measurement duration. The precision of $\Delta^{13}CDH_3$ and $\Delta^{12}CD_2H_2$ is calculated by propagating the error from the measured $\delta^{13}C$, δD, $\delta^{13}CDH_3$ and $\delta^{12}CD_2H_2$ values, using the equations 3c and 3d.

Table 4: Average standard errors of $\delta^{13}C$, δD, $\delta^{13}CDH_3$ and $\delta^{12}CD_2H_2$ measurements on the Ultra and the expected errors from counting statistics of the shot noise. The "factor worse" shows how good our measurements are compared to the shot noise limit.

δ measured on the Ultra	Expected error (‰)	Actual error (‰)	Std dev of error (‰)	Factor worse
$\delta^{13}C$	0.006	0.007	0.002	1.16
δD	0.045	0.110	0.03	2.4
$\delta^{13}CDH_3$	0.293	0.312	0.05	1.06
$\delta^{12}CD_2H_2$	2.22	2.26	0.8	1.03

The measurement procedure is slightly modified for samples smaller than 2 mL of CH_4. In such cases, $^{12}CD_2H_2$ is measured relatively longer than the standard procedure, with shorter measurements of $^{12}CDH_3$ to attain the maximum possible precision for $\Delta^{12}CD_2H_2$.

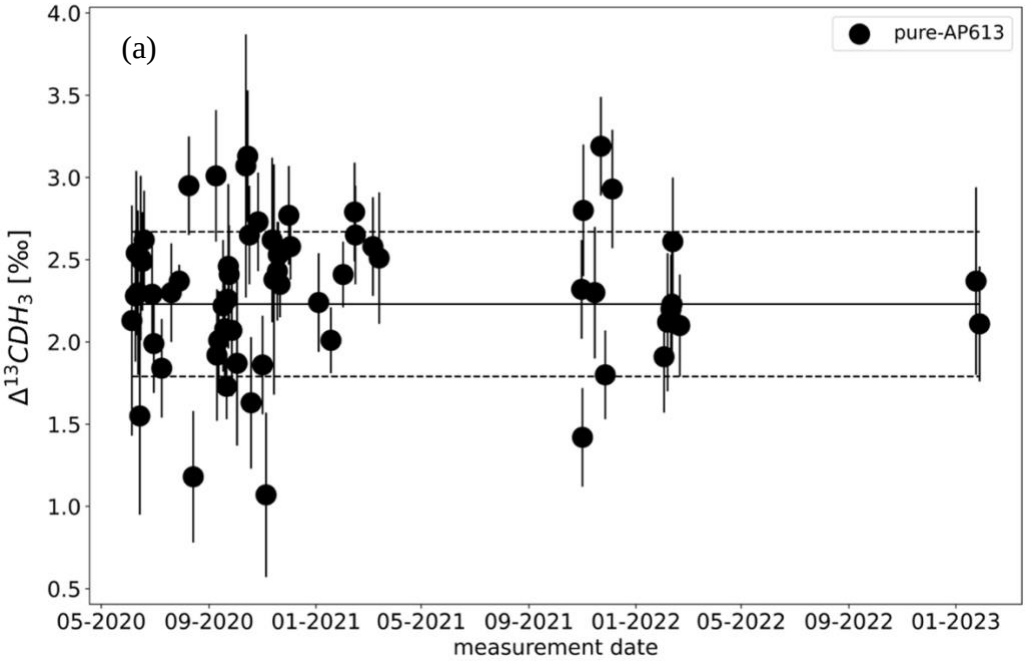

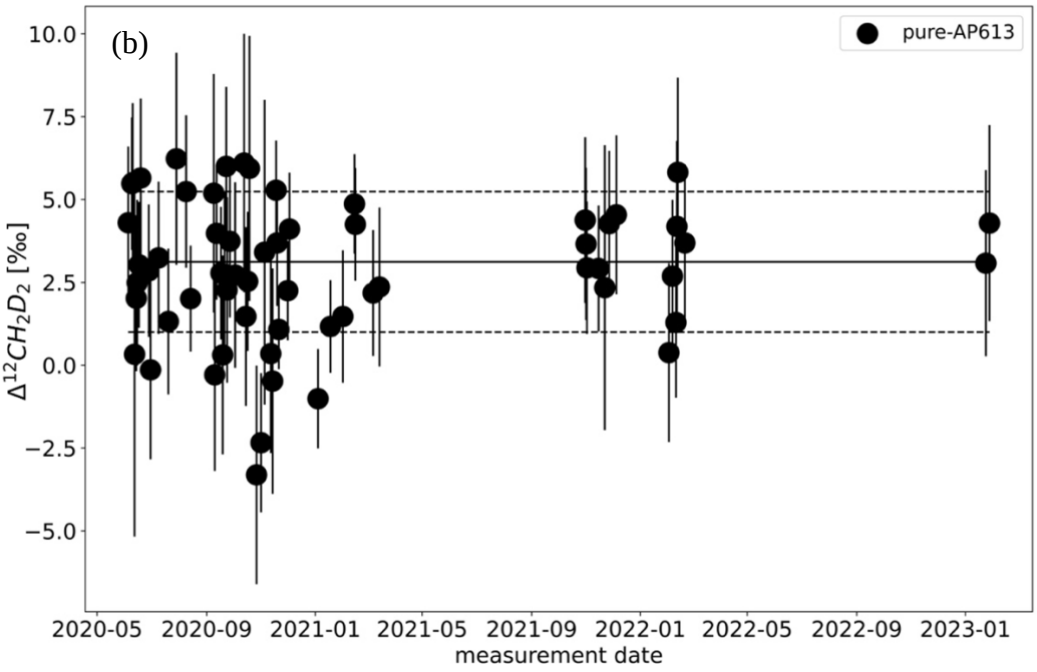

Fig 5: Results of the zero enrichment measurements, each dot representing the calculated clumping anomalies $\Delta^{13}CDH_3$ (a) and $\Delta^{12}CD_2H_2$ (b) of gas AP613. The solid black line represents the values of AP613 assigned from the temperature calibration experiments and the black dashed lines indicate the 1σ std.dev of these measurements over 3 years.

The results of the zero enrichment measurements using AP613 are shown in Fig 5. The mean of these measurements done over 3 years is 2.3 ± 0.1 ‰ for $\Delta^{13}CDH_3$ and 3.2 ± 0.3 ‰ for $\Delta^{12}CD_2H_2$ and all the data points fall symmetrically around the values of AP613 calibrated based on the heating experiments (2.2 ± 0.1 ‰ and 3.1 ± 0.9 ‰ for $\Delta^{13}CDH_3$ and $\Delta^{12}CD_2H_2$ respectively). The standard deviation of these measurements, 0.4 ‰ for $\Delta^{13}CDH_3$ and 2.1 ‰

for $\Delta^{12}CD_2H_2$, is close to the typical measurement error. Together, these measurements show that there are no other large sources of errors in the sample measurements (e.g., leaks in the inlet and/or room temperature variations) and that both bellows used for the measurements behave similarly.

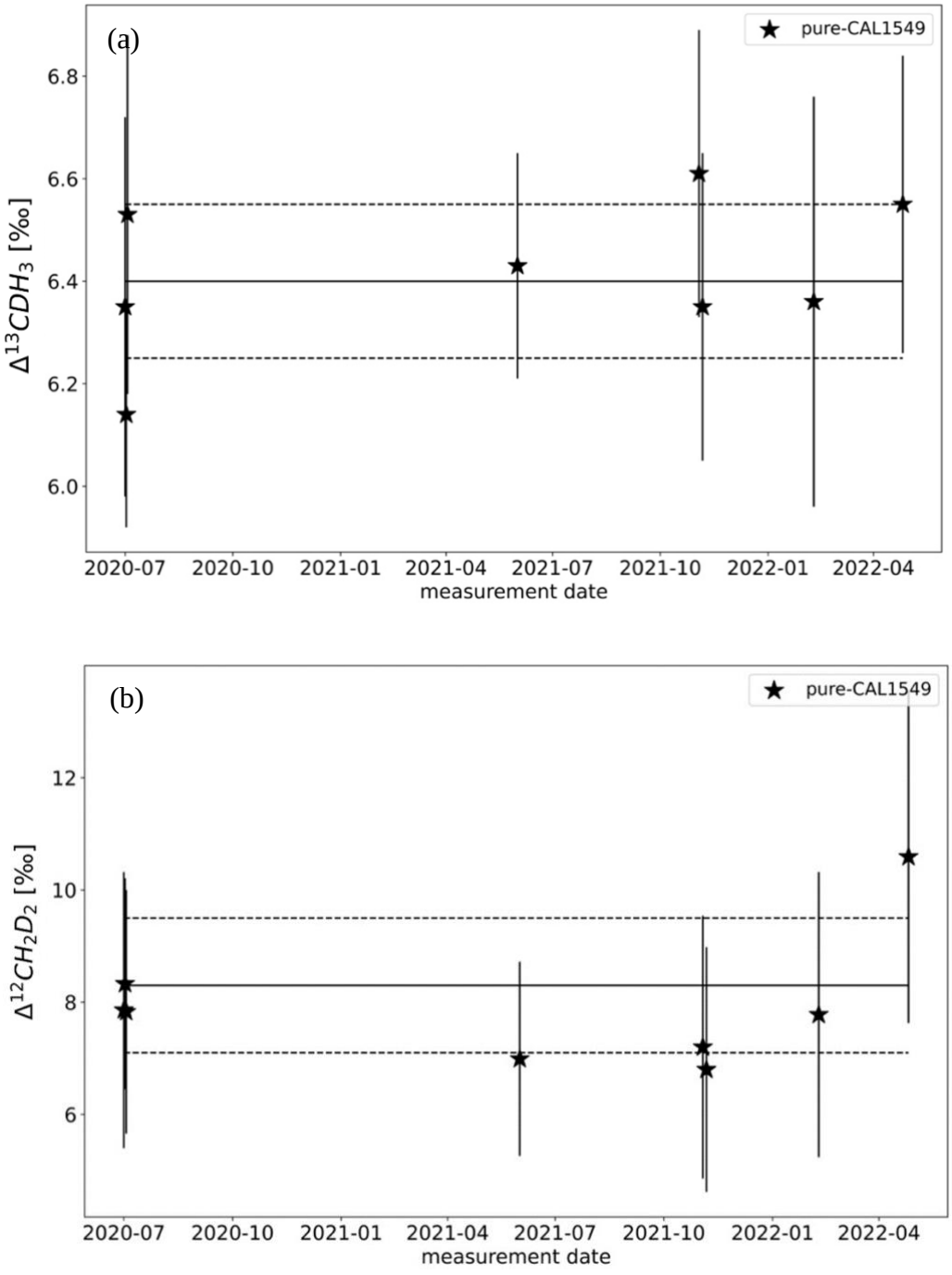

Fig 6: Results of the measurements of pure-CAL1549 for $\Delta^{13}CDH_3$ (a) and $\Delta^{12}CD_2H_2$ (b). The solid black line represents the average value of these measurements, and the black dashed line is the standard deviation (1 σ) of the 8 measurements shown.

The reproducibility of the measurements on the Ultra was quantified by repeated measurements of pure-CAL1549 as shown in Fig 6. Long-term reproducibility, estimated as 1 σ standard deviation of the measurements of pure-CAL1549 over almost 3 years, is around 0.15 ‰ for $\Delta^{13}CDH_3$ and 1.2 ‰ for $\Delta^{12}CD_2H_2$. This external reproducibility is consistent with the individual measurement uncertainty, which is on average 0.3‰ for $\Delta^{13}CDH_3$ and 2.3‰ for $\Delta^{12}CD_2H_2$ for these measurements.

3.4 Inter-laboratory calibration

Three of our gases, AP613, CAL1549 and IMAU-3 were measured on both Thermo Ultra at Utrecht University (UU) and Nu Panorama at University of Maryland (UMD). The results of these measurements are given in Table 5.

Table 5: Comparison of $\Delta^{13}CDH_3$ and $\Delta^{12}CD_2H_2$ measurements of the three reference gases: AP613, CAL1549 and IMAU-3 on the Ultra at UU and the Panorama at UMD.

Gas	$\Delta^{13}CDH_3$ UU (‰)	sd	$\Delta^{13}CDH_3$ UMD (‰)	sd	$\Delta^{12}CD_2H_2$ UU (‰)	sd	$\Delta^{12}CD_2H_2$ UMD (‰)	sd	$\Delta^{13}CDH_3$ difference (‰)	$\Delta^{12}CD_2H_2$ difference (‰)
AP613	2.23	0.12	1.9	0.5	3.12	0.9	3.1	0.8	0.3	0.02
CAL1549	6.4	0.4	6.1	0.5	8.3	2.0	10.0	0.8	0.3	-1.7
IMAU-3	2.5	0.3	1.8	0.5	0.4	1.2	-0.7	0.7	0.6	1.1

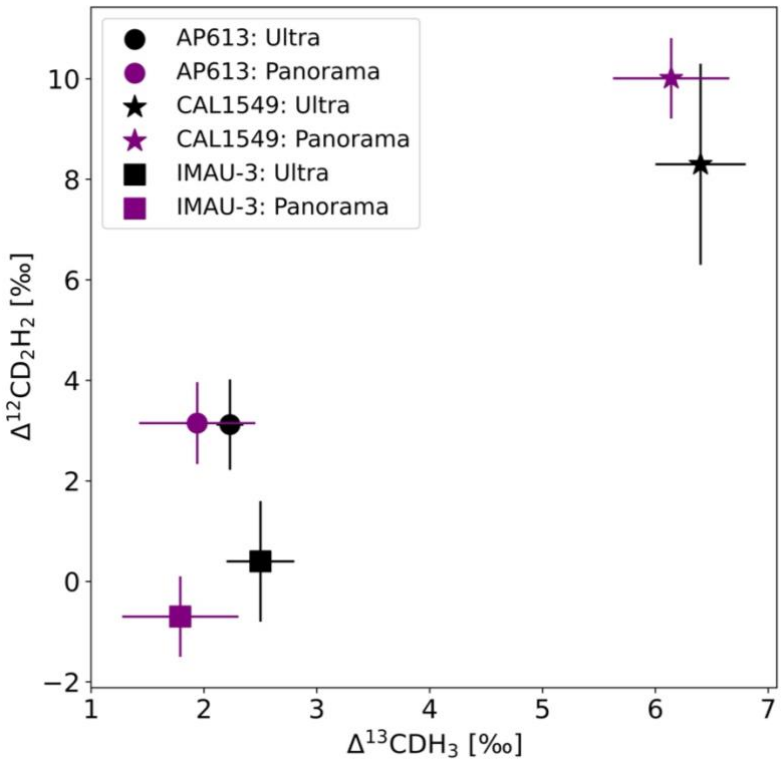

Fig 7: The clumping anomalies of AP613, CAL-1549 and IMAU-3 measured on the UU-Ultra (black) and the UMD-Panorama (purple). The shapes dot, star and square represent the gases AP613, CAL-1549 and IMAU-3 respectively.

The values assigned to AP613 using our heating experiments (section 3.2) agree well with the measured value of the non-heated pure AP613 on the Panorama as shown in Fig 7. The other two gases are also within the measurement uncertainty (1 σ).

3.5 Extraction test with known gas

As mentioned earlier, mixtures of pure CH_4 from AP613 or CAL1549 with zero air were used to test and characterize the extraction system. The CH_4 extracted from these mixtures was measured against the AP613 reference gas on the Ultra. The results of the measurements are presented in Fig 8 as the difference between the expected and the measured values. We expect this difference to be zero within the measurement uncertainty if the extraction procedure doesn't introduce any isotopic fractionation. Pure CH_4 from CAL1549 was also passed through the extraction system (hereby denoted as pure-CAL1549 extracted) using the normal extraction procedure to check for any contamination or fractionation associated with gas introduction and collection via the extraction system.

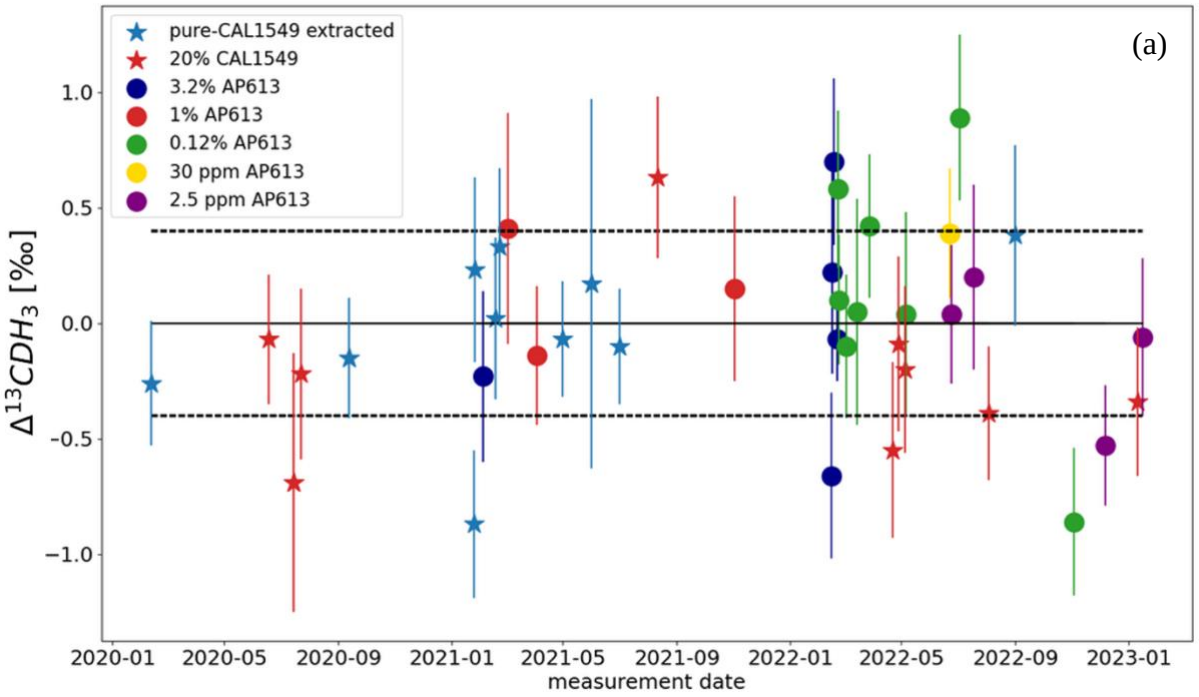

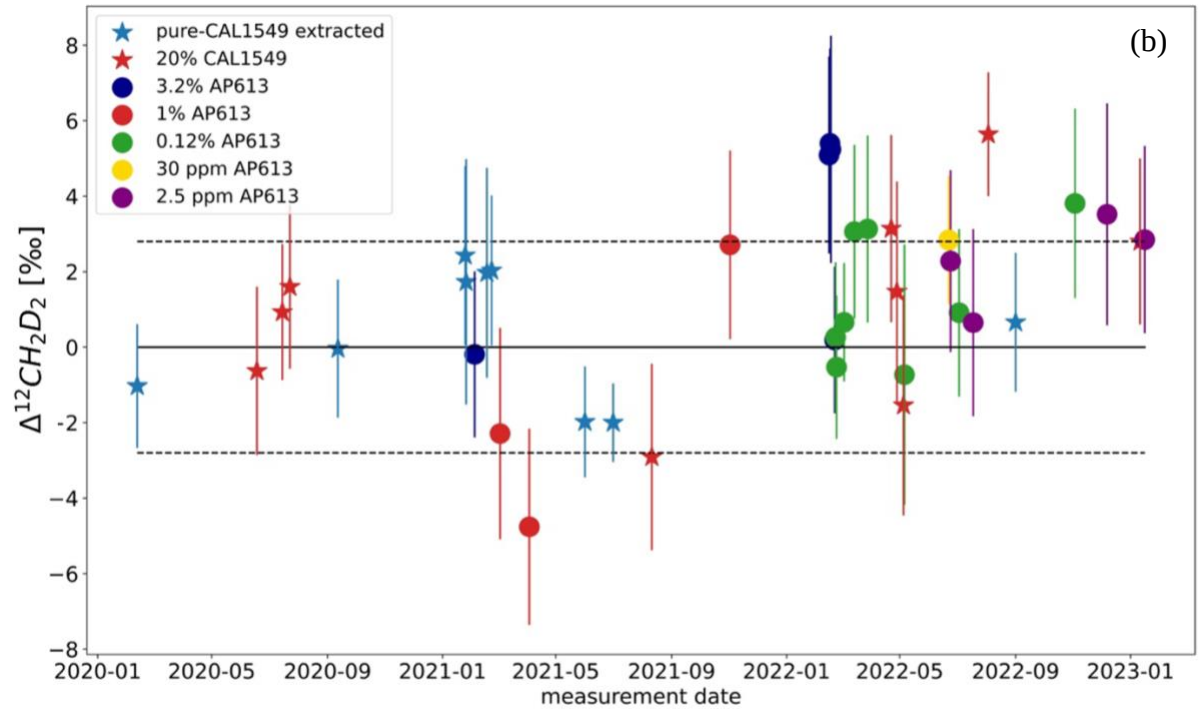

Fig 8: Test results of the extraction system with different mixtures of laboratory reference gasses as stated in the legend. Each coloured dot and star represent the difference between the measured and expected $\Delta^{13}CDH_3$ (a) and $\Delta^{12}CD_2H_2$ (b) values, respectively, of extracted-AP613 and extracted-CAL1549 as given in the legend. The black dashed line is the standard deviation (1 σ) of the difference for $\Delta^{13}CDH_3$ and $\Delta^{12}CD_2H_2$ respectively.

The standard deviation of the difference between the expected and the measured values of these extraction tests are 0.4 ‰ for $\Delta^{13}CDH_3$ and 2.8 ‰ for $\Delta^{12}CD_2H_2$. Most of these

686 extracted reference gas measurements are within this unexpected uncertainty (1 σ). When the
687 difference was more than about 2 σ, additional tests were performed, or parts of the system
688 were replaced or cleaned longer until the measurements were good enough. Typically, large
689 offsets from the expected values are caused by incomplete trapping and releasing of gas from
690 the silica gel used in Traps A and B of HCES. This is solved by conditioning the silica gel for
691 longer (than the standard procedure, section 2.4.1) at 150 °C.
692
693 The effect of Kr on the measurements were investigated using a 1:1 mixture of IMAU-3 and
694 pure Kr. This mixture was directly measured on the Ultra and compared with the values of
695 pure IMAU-3. The $\delta^{13}C$, δD, $\Delta^{13}CDH_3$ and $\Delta^{12}CD_2H_2$ of the mixture measured on the Ultra
696 are -34.6 ‰, -242.0 ‰, 7.45 ± 0.37 ‰, 65.7 ± 2.3 ‰, respectively, whereas that of pure
697 IMAU-3 are -36.6 ‰, -200.0 ‰, 2.5 ± 0.3 ‰, 0.4 ± 1.2 ‰, respectively. This shows that Kr
698 introduces a strong bias on the measurements of both the bulk and clumped isotopic
699 composition of CH_4. Therefore, it is very important to remove Kr from the sample before
700 measuring the CH_4 isotopic composition on the Ultra.
701
702 **3.6. Chromatograms**
703
704 Accurate and precise measurements of $\Delta^{13}CDH_3$ and $\Delta^{12}CD_2H_2$ on the Ultra requires 3 ± 1
705 mL of pure CH_4. CH_4 from sample mixtures pre-concentrated in the extraction system is
706 separated from the bulk sample using the GC, as explained in detail above. Chromatograms
707 for samples with different CH_4 concentrations are illustrated in Fig 9. When the total sample
708 volume is above 100 mL, O_2 and N_2 are not completely separated from CH_4 and therefore, a
709 second round of GC purification is needed (Fig 9b and 9c). For atmospheric CH_4 samples,
710 separation of Kr from CH_4 is attained only when the GC columns are kept at 40 °C (Fig 9e)
711 instead of the usual 50 °C (Fig 9d) used for other CH_4 samples.
712

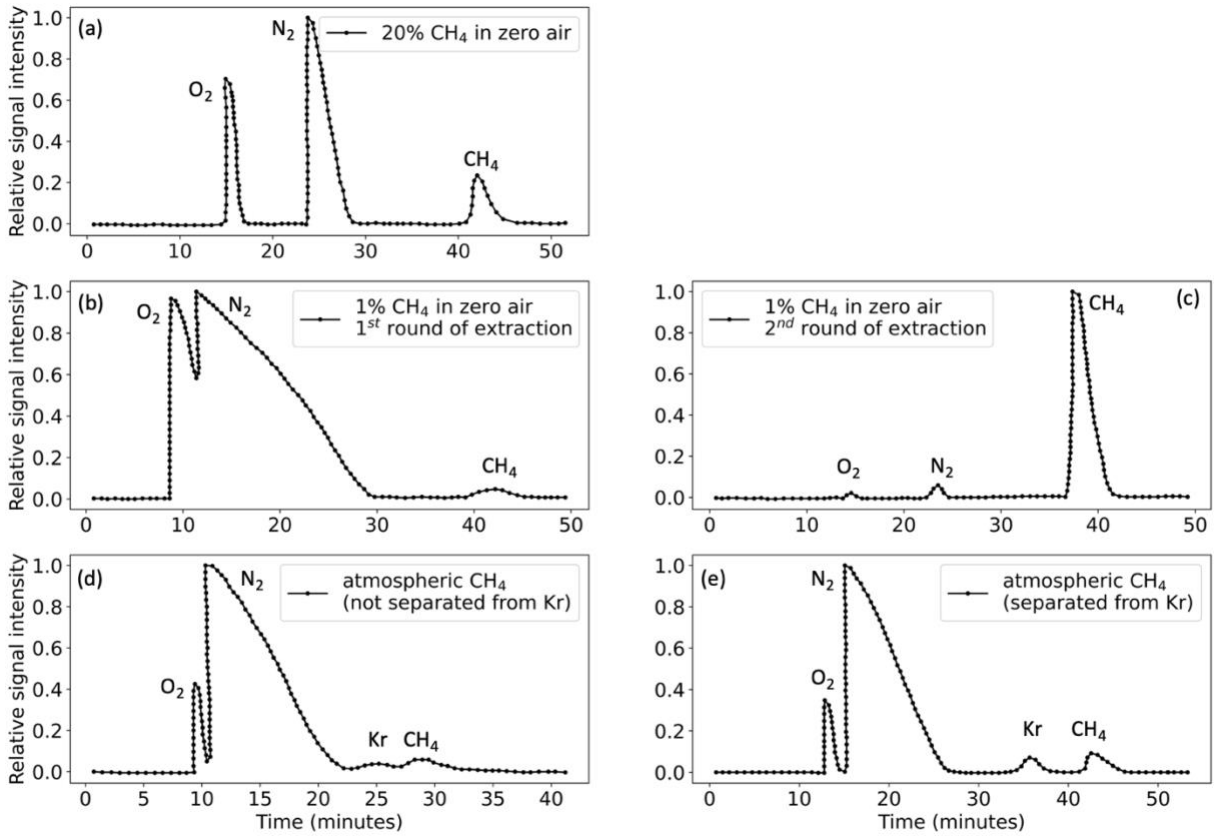

Fig 9: GC chromatograms of different sample mixtures as shown in the legends. (a) chromatogram of 20 % CH_4 + 80 % zero air: 25 mL sample volume (5 mL CH_4). (b) and (c) chromatograms of first and second round of 1 % CH_4 + 99 % zero air: 250 mL sample volume (2.5 mL CH_4). (d) chromatogram of a pre-concentrated atmospheric air: 70 mL sample volume (2 mL CH_4), when GC columns were heated at 50 °C and Kr is not separated from CH_4. (e) chromatogram of pre-concentrated atmospheric air when GC columns were heated at 40 °C and Kr and CH_4 are well separated.

3.7 Propagation of error from clumping anomaly to the formation temperature

The clumping anomalies, $\Delta^{13}CDH_3$ and $\Delta^{12}CD_2H_2$, can be used to calculate the formation temperature of CH_4 when it is formed in thermodynamic equilibrium. The average precision of the Ultra measurements is 0.3 ‰ $\Delta^{13}CDH_3$ and 2.4 ‰ for $\Delta^{12}CD_2H_2$. When propagated into the calculated temperatures (equations 4a and 4b), the measurement error has a non-linear effect across the temperature range of 0–1000 °C. This is because of the polynomial function that defines the relation between the clumping anomalies and temperatures as given in Equation 4a and 4b. Figure 10 shows that the formation temperatures can be predicted with relatively low uncertainty at lower temperatures. For example, at 50 °C the formation temperature can be estimated as 50^{+13}_{-12} °C from $\Delta^{13}CDH_3$ and 50^{+19}_{-17} °C from $\Delta^{12}CD_2H_2$. At 400 °C, for the same measurement precision, the temperature estimated from $\Delta^{13}CDH_3$ is 400^{+90}_{-66} °C and from $\Delta^{12}CD_2H_2$ is 400^{+410}_{-154} °C. Although the absolute clumped isotope effects are larger for $\Delta^{12}CD_2H_2$ than for $\Delta^{13}CDH_3$, formation temperatures calculated from $\Delta^{13}CDH_3$

give a more precise temperature estimate because of the better measurement precision for $\Delta^{13}CDH_3$.

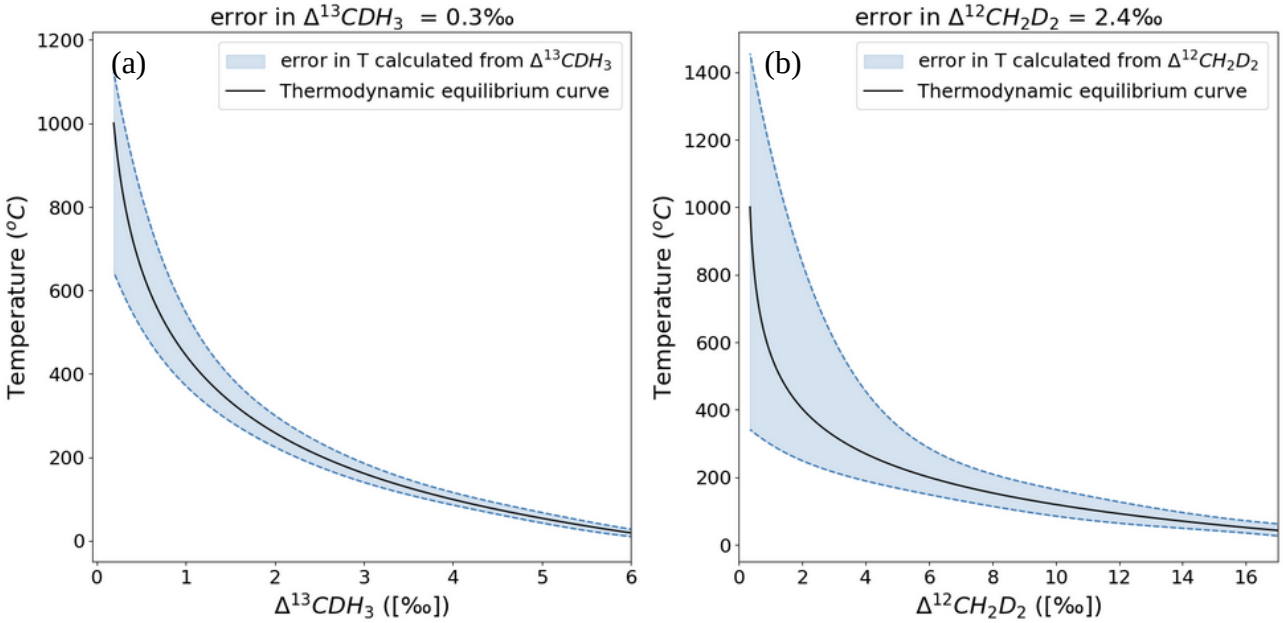

Fig 10: Error in the formation temperatures calculated from $\Delta^{13}CDH_3$ (a) and $\Delta^{12}CD_2H_2$ (b). The black solid line represents the thermodynamic equilibrium curve, and the blue dashed lines give the upper and lower limits of the errors of temperatures propagated from the errors in the measured clumping anomaly.

3.8 Overview of different samples measured.

3.8.1 Samples with different source signatures

CH_4 samples collected from different origins and from laboratory experiments were extracted and measured with the setup explained in section 2.4. An overview of the bulk and clumped isotopic composition of some of these samples from different sources of CH_4 is presented in Fig 11 (Table ST1 in the supplement). The precision of individual measurements is in the range of 0.2 to 0.5 ‰ for $\Delta^{13}CDH_3$ and 1.4 to 4 ‰ for $\Delta^{12}CD_2H_2$ depending on the sample volume.

Most of the samples of thermogenic origin lie on or close to the thermodynamic equilibrium line and therefore, the formation temperature of CH_4 can be calculated for them. All the samples with a microbial origin (e.g., incubation experiments with methanogens, CH_4 from lake water and sediments) have depleted $\Delta^{12}CD_2H_2$ values. The low-temperature abiotic CH_4 also has negative $\Delta^{12}CD_2H_2$. This is in line with previous studies that also show that the production of CH_4 by methanogens and in rocks abiotically at lower temperatures is affected by kinetic fractionation and/or combinatorial effect that leads to negative $\Delta^{12}CD_2H_2$. So far, about 80 samples have been measured on the Ultra from very different origins with clumping anomalies ranging from -1 to 6 ‰ for $\Delta^{13}CDH_3$ and -40 to 45 ‰ for $\Delta^{12}CD_2H_2$.

3.8.2 Ambient air measurement

Using the low-concentration extraction system (LCES), we extracted and measured several samples of atmospheric air sampled in Utrecht and the results of the first measurements are given in Table 6.

Table 6: Results of $\delta^{13}C$, δD, $\Delta^{13}CDH_3$ and $\Delta^{12}CD_2H_2$ of atmospheric CH_4 (air A, B and C) sampled in Utrecht and the comparison of the measured values to the model predictions in Haghnegahdar et al. (2017) and Chung and Arnold (2021).

Samples measured/ Model predictions	$\delta^{13}C$ (‰)	δD (‰)	$\Delta^{13}CDH_3$ (‰)	se	$\Delta^{12}CD_2H_2$ (‰)	se
air A	-48.11	-80.3	0.1	0.4	41.7	2.6
air B	-47.99	-84.5	1.87	0.3	40	2.5
air C	-49.84	-115.7	1.91	0.4	42.3	3.8
Haghnegahdar et al. (2017)			4.6		114	
Chung and Arnold (2021)			3.3		93	

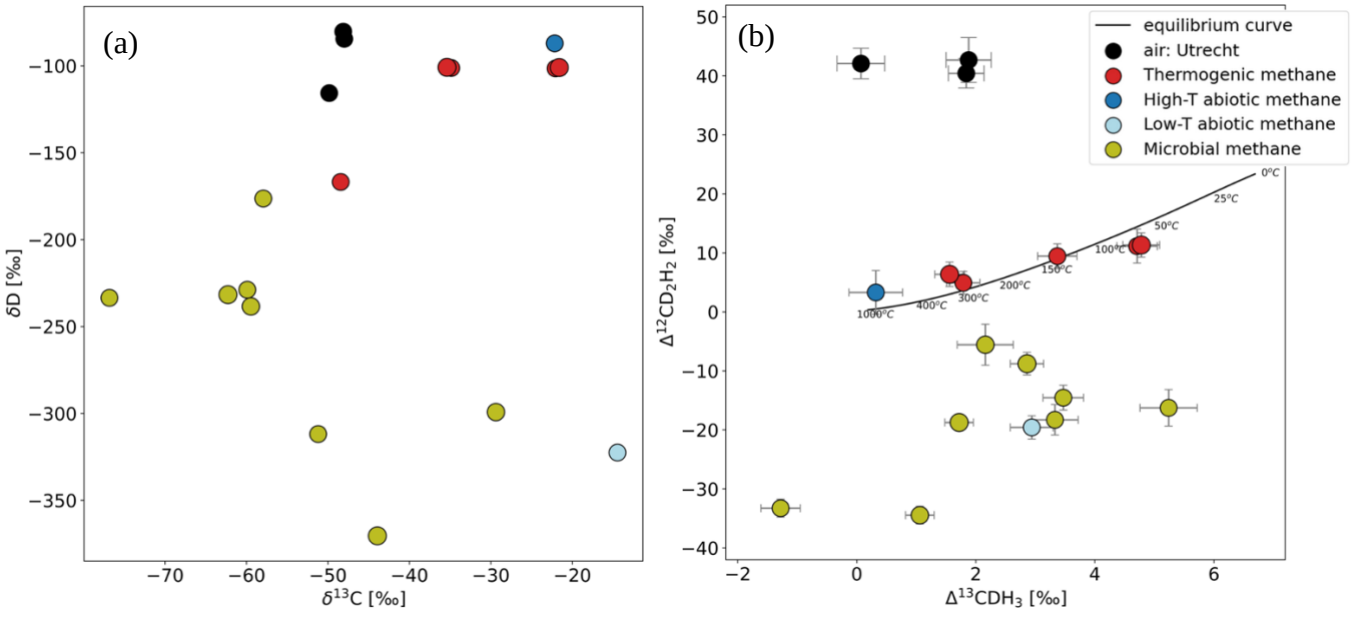

Fig 11: Comparison of $\delta^{13}C$ and δD (a) and $\Delta^{13}CDH_3$ and $\Delta^{12}CD_2H_2$ (b) of samples from different source types and atmospheric air measured outside IMAU. The overview of the samples shown in this figure is given in Table ST1 in the supplement. The solid black line represents the thermodynamic equilibrium curve with corresponding temperature values.

The solid black dots in Fig 11b show the results of the first measurements of the clumping anomaly of atmospheric CH_4 in Utrecht (0-2 ‰ for $\Delta^{13}CDH_3$ and 40-43 ‰ for $\Delta^{12}CD_2H_2$). The air samples in Table 6 were sampled under 3 different atmospheric conditions: (i) clean air from the north (air A); (ii) clean air from the south (air B) and (iii) air with high CH_4 content due to local/regional pollution (air C). The values of the clumped isotopic composition of all three air samples are characterised by a very high anomaly for $\Delta^{12}CD_2H_2$ and a low anomaly for $\Delta^{13}CDH_3$. First measurements of atmospheric methane reported by Haghnegahdar et al. (2023) of air sampled from various atmospheric scenarios in and around Maryland, the USA are compatible (0-3 ‰ for $\Delta^{13}CDH_3$ and 42-55 ‰ for $\Delta^{12}CD_2H_2$) with our measured values.

Firstly, comparing these values to the ones of CH_4 emitted from various sources, it is evident that atmospheric CH_4 has a distinct clumped signature, particularly in $\Delta^{12}CD_2H_2$. The large positive anomaly for $\Delta^{12}CD_2H_2$ of atmospheric CH_4 can be explained by a strong clumped isotope fractionation due to the sink reactions of CH_4 in the atmosphere (Haghnegahdar et al., 2017). The distinct differences between various source types, and the offset of atmospheric CH_4 also suggest that more measurements of the clumping anomaly of air, especially $\Delta^{12}CD_2H_2$, can provide more information about the different sources and sink reactions that determine atmospheric CH_4 levels.

Secondly, the bulk isotopic composition (Table 6) shows as expected lower values for the polluted air C compared to the clean air A and B, indicating regional contributions from biogenic sources as is typical for the Netherlands (Röckmann et al., 2016, Menoud et al., 2021). However, in the case of the clumped isotopes, the air from the north is quite different in $\Delta^{13}CDH_3$, while the values for the polluted and clean air from the south are not very different, unlike the bulk isotopes. At this point we cannot draw strong conclusions, as we only have one measurement per condition and no information on the potential variability. More measurements of $\Delta^{13}CDH_3$ and $\Delta^{12}CD_2H_2$ of air are needed to understand if short-term local / regional atmospheric changes affect the clumping anomaly of air.

Lastly, although the measured $\Delta^{12}CD_2H_2$ of atmospheric CH_4 has very high values compared to the emissions from sources, our measurement results are still far lower than recent model predictions (Chung and Arnold, 2021; Haghnegahdar et al., 2017) (Table 6). The difference can be either due to the inaccuracy in (i) source signatures of all the different sources that contribute to atmospheric CH_4 mole fraction (ii) the theoretical values of kinetic isotopic fractionation factor (KIE) of the sink reactions of CH_4 with OH and Cl and the soil sink reactions.

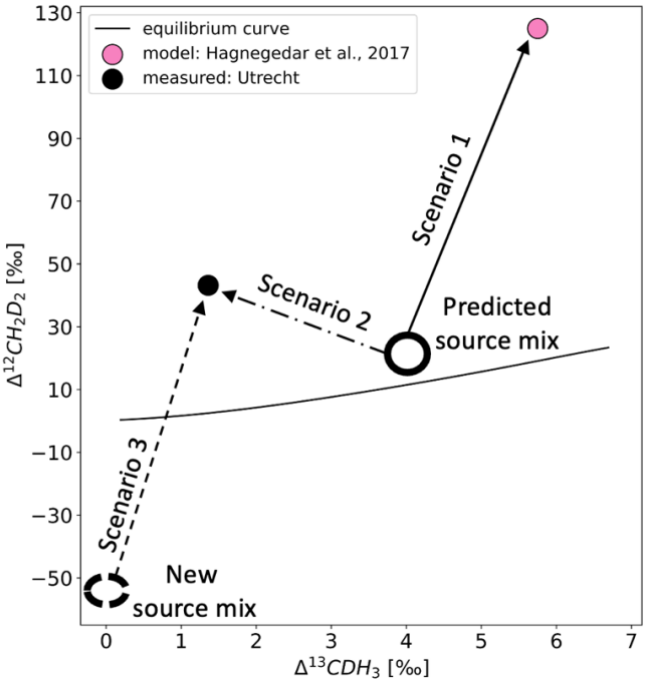

Fig 12: $\Delta^{13}CDH_3$ versus $\Delta^{12}CD_2H_2$ space showing the different scenarios discussed. The solid black line represents the thermodynamic equilibrium curve. The pink dot is the value of air predicted in from the source mix shown as the solid black circle. The black dot is the value of air measured on Ultra. The three arrows show the three scenarios as mentioned in the text. The dashed black circle is the new source mix calculated using Scenario 3.

We used a box model to see how the clumping anomaly of air reacts to these two parameters. The model uses clumping anomalies of the source mixture and the KIEs of OH and Cl sinks as input and gives the expected anomalies of air as output. We work with three scenarios as discussed in detail below and illustrated in Fig 12.

Scenario 1: Replicating the values in the study of Haghnegahdar et al. (2017). If we assume that the predicted clumping anomaly of the mixture of sources in the atmosphere ($\Delta^{13}CDH_3$ = 4 ‰, $\Delta^{12}CD_2H_2$ = 20 ‰) is accurate, then our model also gives higher values of $\Delta^{12}CD_2H_2$ and $\Delta^{13}CDH_3$ of air as in that study, with the same KIE used (OH: 1.92 for $^{12}CD_2H_2$, 1.33 for $^{13}CDH_3$ and Cl: 2.2 for $^{12}CD_2H_2$, 1.46 for $^{13}CDH_3$). This was done to verify that our simple model works well for this study.

Scenario 2: Calculating the KIEs required to arrive at the measured values of air with the same source mix as used in Haghnegahdar et al. (2017). To get the measured values from the predicted source mix, the KIEs must be lowered to 1.79 for $^{12}CD_2H_2$ and 1.325 for $^{13}CDH_3$ for reaction with OH and 1.9 for $^{12}CD_2H_2$ and 1.45 for $^{13}CDH_3$ for reaction with Cl. This relatively small change causes a difference of about 60 ‰ in $\Delta^{12}CD_2H_2$ between the two scenarios 1 and 2. Therefore, the clumping anomalies are very sensitive to the KIEs of the sink reactions.

Scenario 3: Calculating the clumping anomaly of the source mixture that is consistent with the KIEs used in Haghnegahdar et al. (2017) and the atmospheric air measurements presented here. In this case, the clumped isotope anomaly of the source mixture must be heavily depleted, especially in $\Delta^{12}CD_2H_2$ ($\Delta^{13}CDH_3$ = 0‰, $\Delta^{12}CD_2H_2$ = -54‰) to get the measured values using the KIEs in scenario 1. This is much lower than the predicted value and would imply a strong underestimation of CH_4 sources with depleted clumping anomalies such as biogenic sources.

Given the rather high amount of clumped isotope measurements of CH_4 sources that have been published to date, it seems unrealistic that the clumping anomaly of the source mix is so depleted in $\Delta^{12}CD_2H_2$ as calculated in scenario 3, which would imply that the KIE was previously indeed overestimated. These simple isotope mass balance calculations show that we need very precise estimations of the sink KIEs and more accurate measurements of the sources to completely understand the atmospheric CH_4 budget using clumping anomalies.

4. Summary and Conclusion

We have presented a new versatile analytical setup for extraction, sample preparation and measurement of the clumped isotope composition of CH_4 on the Thermo Ultra instrument, including samples at atmospheric concentration. The extraction and GC purification techniques do not cause significant isotopic fractionation and preserve the signatures of the CH_4 source. Currently, the system has been tested and works well for sample volumes of upto 1100 L. The typical precisions of samples measured on the Ultra are 0.3 ± 0.1 ‰ for $\Delta^{13}CDH_3$ and 2.4 ± 0.8 ‰ for $\Delta^{12}CD_2H_2$. The long-term reproducibility, obtained from repeated measurements of pure CAL1549 over almost 3 years, is around 0.15 ‰ for $\Delta^{13}CDH_3$ and 1.2 ‰ for $\Delta^{12}CD_2H_2$. The standard deviation of the difference between the expected and the measured values of all the extraction tests performed are 0.4‰ for $\Delta^{13}CDH_3$ and 2.8 ‰ for $\Delta^{12}CD_2H_2$. The total measurement time is around 20 hours. The system and the measurement procedure can be adjusted to optimise the sample volume required and long measurement times. First measurements of samples from various sources yield results in general agreement with published values. We have measured about 80 samples on the Ultra from very different origins and a wide range of clumping anomalies: -1 – 6 ‰ for $\Delta^{13}CDH_3$ and -40 – 45 ‰ for $\Delta^{12}CD_2H_2$. Our measurements of atmospheric CH_4 show enriched $\Delta^{12}CD_2H_2$ values, but not as high as recently predicted by clumped isotope models. It is unlikely that the discrepancy can be explained only by an underestimation of sources with negative $\Delta^{12}CD_2H_2$, but we show that a small adjustment in the KIEs of the sinks could reconcile atmospheric and source clumped isotope compositions. The precision of atmospheric CH_4 measurements can still be improved by extracting CH_4 from much larger samples (2000 L).

Data availability

Data supporting this study are openly available at: Sivan, Malavika. (2023). Extraction, purification, and clumped isotope analysis of methane (Δ13CDH3 and Δ12CD2H2) from different sources and the atmosphere [Data set]. Zenodo. https://doi.org/10.5281/zenodo.8269713

Competing Interests

The authors declare that they have no conflict of interest.

Author contribution

All authors contributed to the design of the study. M. Sivan undertook the laboratory work with help from C. van der Veen and M. E. Popa. M. Sivan wrote the manuscript with input from all co-authors.

Acknowledgements

We would like to acknowledge the contributions of Dipayan Paul and Sönke Szidat for their important pioneering steps in testing the extraction line and setting up the Ultra measurement procedure. We would like to thank Edward Young for his help building the high concentration extraction line. We would also like to thank Jiayang Sun and James Farquhar from the University of Maryland for the measurements of our reference gases on the Nu Panorama instrument. We also thank our collaborators for contributing to the sample set used in this paper. M. E. Popa, M. Sivan and the Thermo Ultra instrument are supported by the Netherlands Earth Science System Center (NESSC), with funding from the European Union's Horizon 2020 research and innovation programme under the Marie Skłodowska-Curie, grant agreement No 847504.

References

Adnew, G. A., Hofmann, M. E. G., Paul, D., Laskar, A., Surma, J., Albrecht, N., Pack, A., Schwieters, J., Koren, G., Peters, W., and Röckmann, T.: Determination of the triple oxygen and carbon isotopic composition of CO_2 from atomic ion fragments formed in the ion source of the 253 Ultra high-resolution isotope ratio mass spectrometer, Rapid Communications in Mass Spectrometry, 33, 1363-1380, https://doi.org/10.1002/rcm.8478, 2019.

Archer, D., Eby, M., Brovkin, V., Ridgwell, A., Cao, L., Mikolajewicz, U., Caldeira, K., Matsumoto, K., Munhoven, G., Montenegro, A., and Tokos, K.: Atmospheric Lifetime of Fossil Fuel Carbon Dioxide, Annual Review of Earth and Planetary Sciences, 37, 117-134, http://doi.org/10.1146/annurev.earth.031208.100206, 2009.

Assonov, S., Groening, M., Fajgelj, A., Hélie, J. F., and Hillaire-Marcel, C.: Preparation and characterisation of IAEA-603, a new primary reference material aimed at the VPDB scale

realisation for δ(13) C and δ(18) O determination, Rapid Commun Mass Spectrom, 34, e8867, http://doi.org/10.1002/rcm.8867, 2020.

Beck, V., Chen, H., Gerbig, C., Bergamaschi, P., Bruhwiler, L., Houweling, S., Röckmann, T., Kolle, O., Steinbach, J., Koch, T., Sapart, C. J., van der Veen, C., Frankenberg, C., Andreae, M. O., Artaxo, P., Longo, K. M., and Wofsy, S. C.: Methane airborne measurements and comparison to global models during BARCA, Journal of Geophysical Research: Atmospheres, 117, https://doi.org/10.1029/2011JD017345, 2012.

Bergamaschi, P., Bräunlich, M., Marik, T., and Brenninkmeijer, C. A. M.: Measurements of the carbon and hydrogen isotopes of atmospheric methane at Izaña, Tenerife: Seasonal cycles and synoptic-scale variations, Journal of Geophysical Research: Atmospheres, 105, 14531-14546, https://doi.org/10.1029/1999JD901176, 2000.

Bergamaschi, P., Brenninkmeijer, C. A. M., Hahn, M., Röckmann, T., Scharffe, D. H., Crutzen, P. J., Elansky, N. F., Belikov, I. B., Trivett, N. B. A., and Worthy, D. E. J.: Isotope analysis based source identification for atmospheric CH_4 and CO sampled across Russia using the Trans-Siberian railroad, Journal of Geophysical Research: Atmospheres, 103, 8227-8235, https://doi.org/10.1029/97JD03738, 1998.

Cantrell, C. A., Shetter, R. E., McDaniel, A. H., Calvert, J. G., Davidson, J. A., Lowe, D. C., Tyler, S. C., Cicerone, R. J., and Greenberg, J. P.: Carbon kinetic isotope effect in the oxidation of methane by the hydroxyl radical, Journal of Geophysical Research: Atmospheres, 95, 22455-22462, https://doi.org/10.1029/JD095iD13p22455, 1990.

Chung, E. and Arnold, T.: Potential of Clumped Isotopes in Constraining the Global Atmospheric Methane Budget, Global Biogeochemical Cycles, 35, e2020GB006883, https://doi.org/10.1029/2020GB006883, 2021.

Conrad, R.: Control of microbial methane production in wetland rice fields, Nutrient Cycling in Agroecosystems, 64, 59-69, http://doi.org/10.1002/rcm.886710.1023/A:1021178713988, 2002.

Douglas, P. M. J., Stolper, D. A., Eiler, J. M., Sessions, A. L., Lawson, M., Shuai, Y., Bishop, A., Podlaha, O. G., Ferreira, A. A., Santos Neto, E. V., Niemann, M., Steen, A. S., Huang, L., Chimiak, L., Valentine, D. L., Fiebig, J., Luhmann, A. J., Seyfried, W. E., Etiope, G., Schoell, M., Inskeep, W. P., Moran, J. J., and Kitchen, N.: Methane clumped isotopes: Progress and potential for a new isotopic tracer, Organic Geochemistry, 113, 262-282, https://doi.org/10.1016/j.orggeochem.2017.07.016, 2017.

Eiler, J. M.: "Clumped-isotope" geochemistry—The study of naturally-occurring, multiply-substituted isotopologues, Earth and Planetary Science Letters, 262, 309-327, https://doi.org/10.1016/j.epsl.2007.08.020, 2007.

Eiler, J. M., Clog, M., Magyar, P., Piasecki, A., Sessions, A., Stolper, D., Deerberg, M., Schlueter, H.-J., and Schwieters, J.: A high-resolution gas-source isotope ratio mass spectrometer, International Journal of Mass Spectrometry, 335, 45-56, https://doi.org/10.1016/j.ijms.2012.10.014, 2013.

Eldridge, D. L., Korol, R., Lloyd, M. K., Turner, A. C., Webb, M. A., Miller, T. F., III, and Stolper, D. A.: Comparison of Experimental vs Theoretical Abundances of $^{13}CH_3D$ and

$^{12}CH_2D_2$ for Isotopically Equilibrated Systems from 1 to 500 °C, ACS Earth and Space Chemistry, 3, 2747-2764, http://doi.org/10.1021/acsearthspacechem.9b00244, 2019.

Etiope, G. and Sherwood Lollar, B.: ABIOTIC METHANE ON EARTH, Reviews of Geophysics, 51, 276-299, https://doi.org/10.1002/rog.20011, 2013.

Fernandez, J. M., Maazallahi, H., France, J. L., Menoud, M., Corbu, M., Ardelean, M., Calcan, A., Townsend-Small, A., van der Veen, C., Fisher, R. E., Lowry, D., Nisbet, E. G., and Röckmann, T.: Street-level methane emissions of Bucharest, Romania and the dominance of urban wastewater, Atmospheric Environment: X, 13, 100153, https://doi.org/10.1016/j.aeaoa.2022.100153, 2022.

Giunta, T., Young, E. D., Warr, O., Kohl, I., Ash, J. L., Martini, A., Mundle, S. O. C., Rumble, D., Pérez-Rodríguez, I., Wasley, M., LaRowe, D. E., Gilbert, A., and Sherwood Lollar, B.: Methane sources and sinks in continental sedimentary systems: New insights from paired clumped isotopologues 13CH3D and 12CH2D2, Geochimica et Cosmochimica Acta, 245, 327-351, https://doi.org/10.1016/j.gca.2018.10.030, 2019.

Gonfiantini, R.: Standards for stable isotope measurements in natural compounds, Nature, 271, 534-536, http://doi.org/10.1038/271534a0, 1978.

Haghnegahdar, M. A., Schauble, E. A., and Young, E. D.: A model for 12CH2D2 and 13CH3D as complementary tracers for the budget of atmospheric CH4, Global Biogeochemical Cycles, 31, 1387-1407, https://doi.org/10.1002/2017GB005655, 2017.

Haghnegahdar, M. A., Sun, J., Hultquist, N., Hamovit, N. D., Kitchen, N., Eiler, J., Ono, S., Yarwood, S. A., Kaufman, A. J., Dickerson, R. R., Bouyon, A., Magen, C., and Farquhar, J.: Tracing sources of atmospheric methane using clumped isotopes, Proceedings of the National Academy of Sciences, 120, e2305574120, doi:10.1073/pnas.2305574120, 2023.

Kelly, B. F. J., Lu, X., Harris, S. J., Neininger, B. G., Hacker, J. M., Schwietzke, S., Fisher, R. E., France, J. L., Nisbet, E. G., Lowry, D., van der Veen, C., Menoud, M., and Röckmann, T.: Atmospheric methane isotopes identify inventory knowledge gaps in the Surat Basin, Australia, coal seam gas and agricultural regions, Atmos. Chem. Phys., 22, 15527-15558, http://doi.org/10.5194/acp-22-15527-2022, 2022.

Khalil, M. A. K., Shearer, M. J., and Rasmussen, R. A.: Methane Sinks Distribution, Atmospheric Methane: Sources, Sinks, and Role in Global Change, Berlin, Heidelberg, 1993//, 168-179,

Li, Q., Fernandez, R. P., Hossaini, R., Iglesias-Suarez, F., Cuevas, C. A., Apel, E. C., Kinnison, D. E., Lamarque, J.-F., and Saiz-Lopez, A.: Reactive halogens increase the global methane lifetime and radiative forcing in the 21st century, Nature Communications, 13, 2768, http://doi.org/10.1038/s41467-022-30456-8, 2022.

Loyd, S. J., Sample, J., Tripati, R. E., Defliese, W. F., Brooks, K., Hovland, M., Torres, M., Marlow, J., Hancock, L. G., Martin, R., Lyons, T., and Tripati, A. E.: Methane seep carbonates yield clumped isotope signatures out of equilibrium with formation temperatures, Nature Communications, 7, 12274, http://doi.org/10.1038/ncomms12274, 2016.

Lu, X., Harris, S. J., Fisher, R. E., France, J. L., Nisbet, E. G., Lowry, D., Röckmann, T., van der Veen, C., Menoud, M., Schwietzke, S., and Kelly, B. F. J.: Isotopic signatures of major

methane sources in the coal seam gas fields and adjacent agricultural districts, Queensland, Australia, Atmos. Chem. Phys., 21, 10527-10555, http://doi.org/10.5194/acp-21-10527-2021, 2021.

Menoud, M., van der Veen, C., Necki, J., Bartyzel, J., Szénási, B., Stanisavljević, M., Pison, I., Bousquet, P., and Röckmann, T.: Methane (CH_4) sources in Krakow, Poland: insights from isotope analysis, Atmos. Chem. Phys., 21, 13167-13185, http://doi.org/10.5194/acp-21-13167-2021, 2021.

Menoud, M., van der Veen, C., Scheeren, B., Chen, H., Szénási, B., Morales, R. P., Pison, I., Bousquet, P., Brunner, D., and Röckmann, T.: Characterisation of methane sources in Lutjewad, The Netherlands, using quasi-continuous isotopic composition measurements, Tellus B: Chemical and Physical Meteorology, 72, 1-20, http://doi.org/10.1080/16000889.2020.1823733, 2020.

Menoud, M., van der Veen, C., Lowry, D., Fernandez, J. M., Bakkaloglu, S., France, J. L., Fisher, R. E., Maazallahi, H., Stanisavljević, M., Nęcki, J., Vinkovic, K., Łakomiec, P., Rinne, J., Korbeń, P., Schmidt, M., Defratyka, S., Yver-Kwok, C., Andersen, T., Chen, H., and Röckmann, T.: New contributions of measurements in Europe to the global inventory of the stable isotopic composition of methane, Earth Syst. Sci. Data, 14, 4365-4386, http://doi.org/10.5194/essd-14-4365-2022, 2022.

Ono, S., Rhim, J. H., Gruen, D. S., Taubner, H., Kölling, M., and Wegener, G.: Clumped isotopologue fractionation by microbial cultures performing the anaerobic oxidation of methane, Geochimica et Cosmochimica Acta, 293, 70-85, https://doi.org/10.1016/j.gca.2020.10.015, 2021.

Röckmann, T., Popa, M. E., Krol, M. C., and Hofmann, M. E. G.: Statistical clumped isotope signatures, Scientific Reports, 6, 31947, http://doi.org/10.1038/srep31947, 2016a.

Röckmann, T., Eyer, S., van der Veen, C., Popa, M. E., Tuzson, B., Monteil, G., Houweling, S., Harris, E., Brunner, D., Fischer, H., Zazzeri, G., Lowry, D., Nisbet, E. G., Brand, W. A., Necki, J. M., Emmenegger, L., and Mohn, J.: In situ observations of the isotopic composition of methane at the Cabauw tall tower site, Atmos. Chem. Phys., 16, 10469-10487, http://doi.org/10.5194/acp-16-10469-2016, 2016b.

Saueressig, G., Crowley, J. N., Bergamaschi, P., Brühl, C., Brenninkmeijer, C. A. M., and Fischer, H.: Carbon 13 and D kinetic isotope effects in the reactions of CH_4 with O(1 D) and OH: New laboratory measurements and their implications for the isotopic composition of stratospheric methane, Journal of Geophysical Research: Atmospheres, 106, 23127-23138, https://doi.org/10.1029/2000JD000120, 2001.

Sherwood Lollar, B., Lacrampe-Couloume, G., Slater, G. F., Ward, J., Moser, D. P., Gihring, T. M., Lin, L. H., and Onstott, T. C.: Unravelling abiogenic and biogenic sources of methane in the Earth's deep subsurface, Chemical Geology, 226, 328-339, https://doi.org/10.1016/j.chemgeo.2005.09.027, 2006.

Sherwood, O. A., Schwietzke, S., Arling, V. A., and Etiope, G.: Global Inventory of Gas Geochemistry Data from Fossil Fuel, Microbial and Burning Sources, version 2017, Earth Syst. Sci. Data, 9, 639-656, http://doi.org/10.5194/essd-9-639-2017, 2017.

Stolper, D. A., Lawson, M., Formolo, M. J., Davis, C. L., Douglas, P. M. J., and Eiler, J. M.: The utility of methane clumped isotopes to constrain the origins of methane in natural gas accumulations, Geological Society, London, Special Publications, 468, 23-52, http://doi.org/10.1144/SP468.3, 2018.

Stolper, D. A., Sessions, A. L., Ferreira, A. A., Santos Neto, E. V., Schimmelmann, A., Shusta, S. S., Valentine, D. L., and Eiler, J. M.: Combined 13C–D and D–D clumping in methane: Methods and preliminary results, Geochimica et Cosmochimica Acta, 126, 169-191, https://doi.org/10.1016/j.gca.2013.10.045, 2014.

Topp, E. and Pattey, E.: Soils as sources and sinks for atmospheric methane, Canadian Journal of Soil Science, 77, 167-177, http://doi.org/10.4141/s96-107, 1997.

Wang, D. T., Gruen, D. S., Lollar, B. S., Hinrichs, K. U., Stewart, L. C., Holden, J. F., Hristov, A. N., Pohlman, J. W., Morrill, P. L., Könneke, M., Delwiche, K. B., Reeves, E. P., Sutcliffe, C. N., Ritter, D. J., Seewald, J. S., McIntosh, J. C., Hemond, H. F., Kubo, M. D., Cardace, D., Hoehler, T. M., and Ono, S.: Methane cycling. Nonequilibrium clumped isotope signals in microbial methane, Science, 348, 428-431, http://doi.org/10.1126/science.aaa4326, 2015.

Whitehill, A. R., Joelsson, L. M. T., Schmidt, J. A., Wang, D. T., Johnson, M. S., and Ono, S.: Clumped isotope effects during OH and Cl oxidation of methane, Geochimica et Cosmochimica Acta, 196, 307-325, http://doi.org/10.1016/j.gca.2016.09.012, 2017.

Whiticar, M. and Schaefer, H.: Constraining past global tropospheric methane budgets with carbon and hydrogen isotope ratios in ice, Philosophical Transactions of the Royal Society A: Mathematical, Physical and Engineering Sciences, 365, 1793-1828, http://doi.org/10.1098/rsta.2007.2048, 2007.

Whiticar, M. J.: Carbon and hydrogen isotope systematics of bacterial formation and oxidation of methane, Chemical Geology, 161, 291-314, https://doi.org/10.1016/S0009-2541(99)00092-3, 1999.

Whiticar, M. J., Faber, E., and Schoell, M.: Biogenic methane formation in marine and freshwater environments: CO_2 reduction vs. acetate fermentation—Isotope evidence, Geochimica et Cosmochimica Acta, 50, 693-709, https://doi.org/10.1016/0016-7037(86)90346-7, 1986.

Yeung, L. Y.: Combinatorial effects on clumped isotopes and their significance in biogeochemistry, Geochimica et Cosmochimica Acta, 172, 22-38, http://doi.org/10.1016/j.gca.2015.09.020, 2016.

Young, E. D., Kohl, I. E., Sherwood Lollar, B., Etiope, G., Rumble, D., Li, S., Haghnegahdar;, M. A., Schauble;, E. A., McCain;, K. A., Foustoukos;, D. I., Sutclife;, C., Warr;, O., Ballentine;, C. J., Onstott;, T. C., Hosgormez;, H., Neubeck;, A., Marques;, J. M., Pérez-Rodríguez;, I., Rowe;, A. R., LaRowe;, D. E., Magnabosco;, C., Yeung;, L. Y., Ash;, J. L., and Bryndzia, L. T.: The relative abundances of resolved $^{12}CH_2D_2$ and $^{13}CH_3D$ and mechanisms controlling isotopic bond ordering in abiotic and biotic methane gases, Geochimica et Cosmochimica Acta, 203, 235-264, https://doi.org/10.1016/j.gca.2016.12.041, 2017.

1098